

A comprehensive survey on deep active learning and its applications in medical image analysis

Haoran Wang^{a,b}, Qiuye Jin^c, Shiman Li^{a,b}, Siyu Liu^{a,b}, Manning Wang^{a,b,*}, Zhijian Song^{a,b,*}

^aDigital Medical Research Center, School of Basic Medical Sciences, Fudan University, Shanghai 200032, China

^bShanghai Key Laboratory of Medical Image Computing and Computer Assisted Intervention, Shanghai 200032, China

^cComputational Bioscience Research Center (CBRC), King Abdullah University of Science and Technology (KAUST), Thuwal 23955, Saudi Arabia

Abstract

Deep learning has achieved widespread success in medical image analysis, leading to an increasing demand for large-scale expert-annotated medical image datasets. Yet, the high cost of annotating medical images severely hampers the development of deep learning in this field. To reduce annotation costs, active learning aims to select the most informative samples for annotation and train high-performance models with as few labeled samples as possible. In this survey, we review the core methods of active learning, including the evaluation of informativeness and sampling strategy. For the first time, we provide a detailed summary of the integration of active learning with other label-efficient techniques, such as semi-supervised, self-supervised learning, and so on. Additionally, we also highlight active learning works that are specifically tailored to medical image analysis. In the end, we offer our perspectives on the future trends and challenges of active learning and its applications in medical image analysis.

Keywords: Active Learning, Medical Image Analysis, Survey, Deep Learning

1. Introduction

Medical imaging visualizes anatomical structures and pathological processes. It also offers crucial information in lesion detection, diagnosis, treatment planning, and surgical intervention. In recent years, the rise of artificial intelligence (AI) has led to significant success in medical image analysis. The AI-powered systems for medical image analysis have not only approached but even exceeded the performance of human experts in certain clinical tasks. Notable examples include skin cancer classification (Esteva et al., 2017), lung cancer screening with CT scans (Ardila et al., 2019), polyp detection during colonoscopy (Wang et al., 2018), and prostate cancer tissue detection in whole-slide images (Tolkach et al., 2020). Therefore, these AI-powered systems can be integrated into existing clinical workflows, which helps to improve diagnostic accuracy for clinical experts (Sim et al., 2020) and support less-experienced clinicians (Tschandl et al., 2020).

Deep learning (DL) models serve as the core of these AI-powered systems for learning complex patterns from raw images and generalizing them to more unseen cases. The success of DL often relies on large-scale human-annotated datasets. For example, the ImageNet dataset (Deng et al., 2009) contains tens of millions of labeled images, and it's widely used in developing DL models for computer vision. The size of medical image datasets keeps expanding, but it is still relatively smaller than that of natural image datasets. For example, the brain tumor segmentation dataset BraTS (Menze

et al., 2014; Baid et al., 2021) consists of 3D multi-sequence MRI scans. The BraTS dataset expanded from 65 patients in 2013 to over 1,200 in 2021. The latter is equivalent to more than 700,000 annotated 2D images. However, the high annotation cost limits the construction of large-scale medical image datasets, mainly reflected in the following two aspects:

1. Fine-grained annotation of medical images is labor-intensive and time-consuming. In clinical practice, automatic segmentation helps clinicians outline different anatomical structures and lesions more accurately. However, training such a segmentation model requires pixel-wise annotation, which is extremely tedious (Rajpurkar et al., 2022). Another case is in digital pathology. Pathologists usually require detailed examinations and interpretations of pathological tissue slices under high-magnification microscopes. Due to the complex tissue structures, pathologists must continuously adjust the microscope's magnification. As a result, it usually takes 15 to 30 minutes to examine a single slide (Qu et al., 2022). Making accurate annotations is even more challenging for pathologists. In conclusion, the annotation process in medical image analysis demands a considerable investment of time and labor.

2. The high bar for medical image annotation leads to high costs. In computer vision, tasks like object detection and segmentation also require many fine-grained annotations. However, the widespread use of crowdsourcing platforms has significantly reduced the cost of obtaining high-quality annotations in these tasks (Kovashka et al., 2016). However, crowdsourcing platforms have certain limitations in annotating medical images. Firstly, annotating medical images demands both medical knowledge and clinical expertise. Some complex

*Corresponding authors: Manning Wang and Zhijian Song (Emails: hrwang20@fudan.edu.cn, mnwang@fudan.edu.cn, zjsong@fudan.edu.cn)

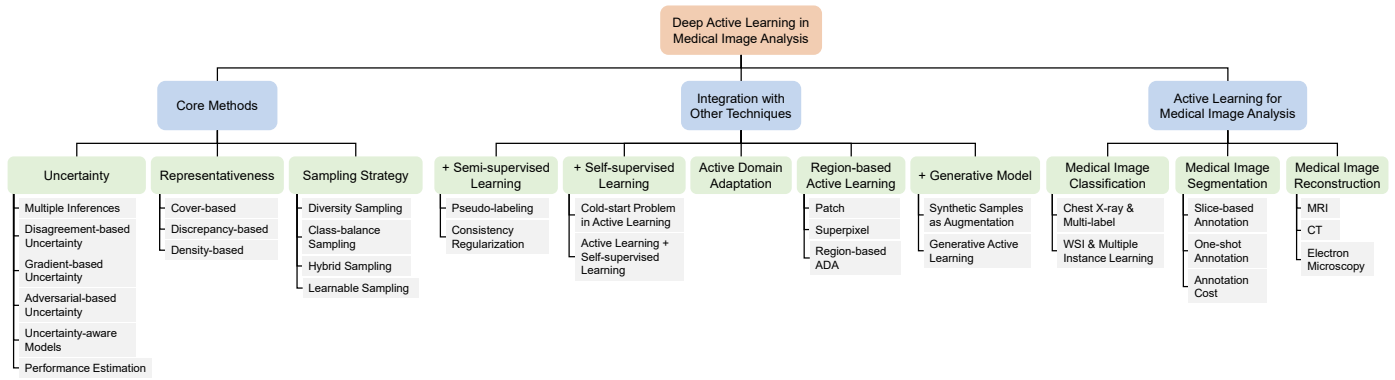


Figure 1: Overall framework of this survey.

cases even require discussions among multiple senior experts. Secondly, even in some relatively simple tasks, crowdsourcing workers tend to provide annotations of poorer quality than professional annotators in medical image analysis. For example, results in Rädtsch et al. (2023) supported the conclusion above in annotating the segmentation mask of surgical instruments. Finally, crowdsourcing platforms may also raise privacy concerns (Rajpurkar et al., 2022). In summary, high-quality annotations often require the involvement of experienced doctors, which inherently increases the annotation cost of medical images.

The high annotation cost is one of the major bottlenecks of DL in medical image analysis. Active learning (AL) is considered one of the most effective solutions for reducing annotation costs. The main idea of AL is to select the most informative samples for annotation and then train a model with these samples in a supervised way. In the general practice of AL, annotating a part of the dataset could reach comparable performance of annotating all samples. As a result, AL saves the annotation costs by querying as few informative samples for annotation as possible. Specifically, we refer to the AL works focusing on training a deep model as deep active learning.

Reviewing AL works in medical image analysis is essential for reducing annotation costs. There are already some surveys on AL in machine learning or computer vision. Settles (2009) provided a general introduction and comprehensive review of AL works in the machine learning era. After the advent of DL, Ren et al. (2021) reviewed the development of deep active learning and its applications in computer vision and natural language processing. Liu et al. (2022b) summarized the model-driven and data-driven sample selectors in deep active learning. Zhan et al. (2022) reimplemented high-impact works in deep active learning with fair comparisons. Takezoe et al. (2023) reviewed recent developments of deep active learning in computer vision and its industrial applications. Regarding related surveys in medical image analysis, Budd et al. (2021) investigated the role of humans in developing and deploying DL in medical image analysis, where AL is considered a vital part of this process. In Tajbakhsh et al. (2020), AL was one of the solutions for training high-performance medical image

segmentation models with imperfect annotation. As one of the methods in label-efficient deep learning for medical image analysis, Jin et al. (2023a) summarized AL methods from model and data uncertainty.

However, the surveys mentioned above have certain limitations. First, new ideas and methods are constantly emerging with the rapid development of deep active learning. Thus, a more comprehensive survey of AL is needed to cover the latest advancements. Second, a recent trend is combining AL with other label-efficient techniques, which is also highlighted as a future direction by related surveys (Takezoe et al., 2023; Budd et al., 2021). However, existing surveys still lack summaries and discussions on this topic. Finally, the high annotation cost emphasizes the increased significance of AL in medical image analysis, yet related reviews still lack comprehensiveness in this regard.

This survey comprehensively reviews AL for medical image analysis, including core methods, integration with other label-efficient techniques, and AL works tailored to medical image analysis. We first searched relevant papers on Google Scholar and arXiv platforms using the keyword “Active Learning” and expanded the search scope through citations. It should be noted that the included papers in this survey mainly belong to the fields of medical image analysis and computer vision. AL works on language, time series, tabular data, and graphs are less emphasized. Additionally, most works in this survey are published in top-tier journals (including TPAMI, TMI, MedIA, JBHI, etc.) and conferences (including CVPR, ICCV, ECCV, ICML, ICLR, NeurIPS, MICCAI, ISBI, MIDL, etc.). As a result, this survey involves nearly 164 relevant AL works with 234 references. The contributions of this paper are summarized as follows:

- Through an exhaustive literature search, we provide a comprehensive review and a novel taxonomy for AL works, especially those focusing on medical image analysis.
- While previous surveys mainly focus on evaluating informativeness, we further summarize different sampling strategies in deep active learning, such as diversity and class-balance strategies, aiming to provide

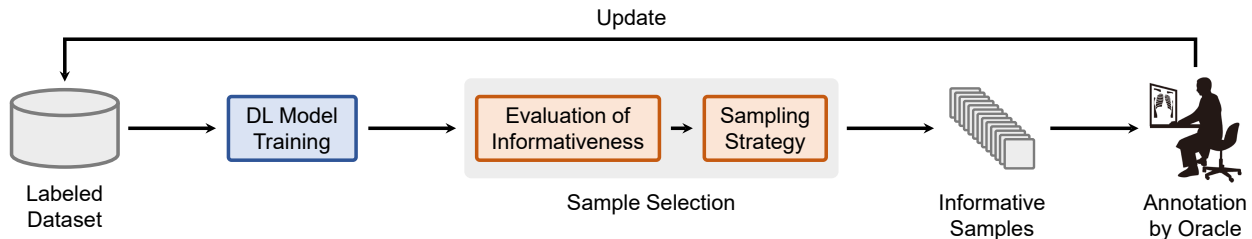


Figure 2: Illustration of the process of active learning.

references for future method improvement.

- In line with current trends, this survey is the first to provide a detailed review of the integration of AL with other label-efficient techniques, including semi-supervised learning, self-supervised learning, domain adaptation, region-based active learning, and generative models.

The rest of this survey is organized as follows: §2 introduces problem settings and mathematical formulation of AL, §3 discusses the core methods of AL, including evaluation of informativeness (§3.1 & §3.2) and sampling strategies (§3.3), §4 reviews the integration of AL with other label-efficient techniques, §5 summarizes AL works tailored to medical image analysis. We discuss existing challenges and future directions of AL in §6 and conclude the whole paper in §7. The overall framework of this survey is shown in Fig. 1.

Due to the rapid development of AL, many related works are not covered in this survey. We refer readers to our constantly updated website¹ for the latest progress of AL and its application in medical image analysis.

2. Problem Settings and Formulations of Active Learning

AL generally involves three problem settings: membership query synthesis, stream-based selective sampling, and pool-based active learning (Settles, 2009). In the case of membership query synthesis, we can continuously query any samples in the input space for annotation, including synthetic samples produced by generative models (Angluin, 1988, 2004). We also refer to this setting as generative active learning in this survey. Membership query synthesis is typically suitable for low-dimensional input spaces. However, when expanded to high-dimensional spaces (e.g., images), the queried samples produced by generative models could be unidentifiable for human labelers. The recent advances of deep generative models have shown great promise in synthesizing realistic medical images, and we further discuss its combination with AL in §4.5. Stream-based selective sampling assumes that samples arrive one by one in a continuous stream, and we need to decide whether or not to request annotation for incoming samples (Cohn et al., 1994).

This setting is suitable for scenarios with limited memory, such as edge computing, but it neglects sample correlations.

Most AL works follow pool-based active learning, which draw samples from a large pool of unlabeled data and requests oracle (e.g., doctors) for annotations. Moreover, if multiple samples are selected for labeling at once, we can further call this setting “batch-mode”. Deep active learning is in batch-mode by default since retraining the model every time a sample is labeled is impractical. Also, one labeled sample may not necessarily result in significant performance improvement. Therefore, unless otherwise specified, all works in this survey follow the setting of batch-mode pool-based active learning.

The flowchart of active learning is illustrated in Fig. 2. Assuming a total of T annotation rounds, active learning primarily consists of the following steps:

1. Sample Selection: In the t -th round of annotation, $1 \leq t \leq T$, an acquisition function A is used to evaluate the informativeness of each sample in the unlabeled pool D_t^u . Then, a batch of samples is selected with a certain sampling strategy S . Specifically, the queried dataset of t -th round D_t^q is constructed as follow:

$$D_t^q = S_{D_t^q \subset D_t^u} \left(A_{x \in D_t^u} (x, f_{\theta_{t-1}}), b \right) \quad (1)$$

where x represents sample in the dataset, D_t^u and D_t^q are unlabeled and queried dataset in round t , respectively. $f_{\theta_{t-1}}$ and θ_{t-1} represent the deep model and its parameters from the previous round, respectively. The annotation budget b is the number of queried samples for each round, far less than the total count of unlabeled samples, i.e., $b = |D_t^q| \ll |D_t^u|$.

2. Annotation by Oracle: After sample selection, the queried set D_t^q is sent to oracle (e.g., doctors) for annotation, and newly labeled samples are added into the labeled dataset D_t^l . The update of D_t^l is as follow:

$$D_t^l = D_{t-1}^l \cup \{(x, y) | x \in D_t^q\} \quad (2)$$

where y represents the label of x , and D_t^l and D_{t-1}^l denote the labeled sets for round t and the previous round, respectively. Besides, the queried samples should be removed from the unlabeled set D_t^u :

$$D_t^u = D_{t-1}^u \setminus \{(x, y) | x \in D_t^q\} \quad (3)$$

3. DL Model Training: After oracle annotation, we train the deep model using the labeled set of this round D_t^l in a fully

¹<https://github.com/LightersWang/Awesome-Active-Learning-for-Medical-Image-Analysis>

supervised manner. The deep model f_{θ_t} is trained on D_t^l to obtain the optimal parameters θ_t for round t . The mathematical formulation is as follows:

$$\theta_t = \arg \min_{\theta} \mathbb{E}_{(x,y) \in D_t^l} [\mathcal{L}(f_{\theta}(x), y)] \quad (4)$$

where \mathcal{L} represents the loss function.

4. Repeat steps 1 to 3 until the annotation budget limit is reached.

It is worth noting that the model needs proper initialization to start the AL process. If the initial model f_{θ_0} is randomly initialized, it could only produce meaningless informativeness. To address this issue, most AL works randomly choose some samples as initially labeled dataset D_0^l and train f_{θ_0} upon D_0^l . For more details on better initialization of AL using pre-trained models, please refer to §4.2.

3. Core Methods of Active Learning

In this survey, we consider the evaluation of informativeness and sampling strategy as the core methods of AL. Informativeness represents the value of annotating each sample. Higher informativeness indicates a higher priority to request these samples for labeling. Typical metrics of informativeness include uncertainty based on model prediction and representativeness based on data distribution. On the other hand, the sampling strategy is used to select a small number of unlabeled samples for annotation based on their informativeness metrics. Common sampling strategies include top-k selection and clustering, etc. Unlike previous surveys, we explicitly define sampling strategies as core methods of AL for the first time. The rationale is that if a perfect informativeness metric existed, one could simply select the samples with the highest value of the informativeness metric according to the annotation budget. However, current informativeness metrics are more or less flawed to some extent. For instance, redundant and class-imbalanced queries are common issues in AL. We need specific sampling strategies to mitigate the issues arising from imperfect informativeness metrics. In this section, we reviewed uncertainty (§3.1), informativeness (§3.2) and sampling strategy (§3.3). Additionally, we provide a summarization of all works in this survey. Methods and basic metrics of calculating uncertainty or representativeness and sampling strategies are detailed in Table 2.

3.1. Evaluation of Informativeness: Uncertainty

Uncertainty is used to assess the reliability of model predictions, with higher uncertainty indicating the model may be more prone to errors (Kendall and Gal, 2017). During sample selection in AL, it is challenging to determine the correctness of the model’s predictions. Nevertheless, we can highlight samples where the model is prone to making errors by uncertainty estimation. Uncertain samples often contain knowledge about the model that has not yet been mastered. Annotating them can improve the performance. Therefore,

Table 1: Formulations of Uncertainty Metrics based on Prediction Probability. x stands for sample, f is the deep model, while C is the number of classes.

Name	Equations
Prediction Probability	$p = \text{Softmax}(f(x)) \in \mathbb{R}^C, p = [p_1, p_2, \dots, p_C]$
Least Confidence	$1 - \max_i p_i$
Entropy	$-\sum_{i=1}^C p_i \log p_i$
Margin	$\max_i p_i - \max_{j \neq k} p_j, k = \arg \max_i p_i$
Mean Variance	$-\frac{1}{C} \sum_{i=1}^C (p_i - \bar{p})^2, \bar{p} = -\frac{1}{C} \sum_{i=1}^C p_i$

uncertainty has become one of the most commonly used informativeness metrics in AL.

The most straightforward uncertainty metrics are based on prediction probabilities, including least confidence (Lewis and Catlett, 1994), entropy (Joshi et al., 2009), margin (Roth and Small, 2006), and mean variance (Gal et al., 2017). These metrics have been widely used in traditional AL, and their formulations are detailed in Table 1. Confidence is the probability of the highest predicted class. We often adopt the least confidence to measure uncertainty, meaning lower confidence indicates higher uncertainty. Entropy is the most common measure of uncertainty, with higher entropy indicating higher uncertainty. The margin represents the difference between the highest and the second-highest predicted probability, with a larger margin indicating greater uncertainty. Besides, a larger mean variance indicates higher uncertainty.

The above uncertainty metrics only require a single forward pass in deep learning. However, due to the notorious issue of over-confidence in deep neural networks (Guo et al., 2017), they cannot be directly transferred to deep AL. In deep learning, over-confidence refers to the model having excessively high confidence in its predictions, even though they might not be accurate. Over-confidence results in high confidence (e.g., 0.99) of the wrong class for misclassified samples. For uncertain samples, it may lead to extreme confidence (e.g., 0.99 or 0.01) instead of normal one (e.g., 0.6 or 0.4) as it should. Over-confidence may cause distorted uncertainty since it affects the predicted probabilities for all classes. This section divides the uncertainty-based AL into multiple inference, disagreement-based uncertainty, uncertainty-aware models, gradient-based uncertainty, adversarial-based uncertainty, and performance estimation. The first three are primarily based on prediction probabilities, while the latter three mostly employ other statistics of deep models for uncertainty estimation. The taxonomy of uncertainty-based AL is shown in Fig. 3.

3.1.1. Multiple Inferences

To mitigate over-confidence, a common strategy is to run the model multiple times with some perturbations and calculate the classic uncertainty metrics with the mean probability. The main idea is to reduce the bias introduced by network architectures or training data. These biases often contribute to the over-confidence issue. Three methods can be employed for multiple inferences: Monte Carlo dropout (MC dropout), model ensemble, and data augmentation. The first two perturb the model parameters, and the last perturb the input data.

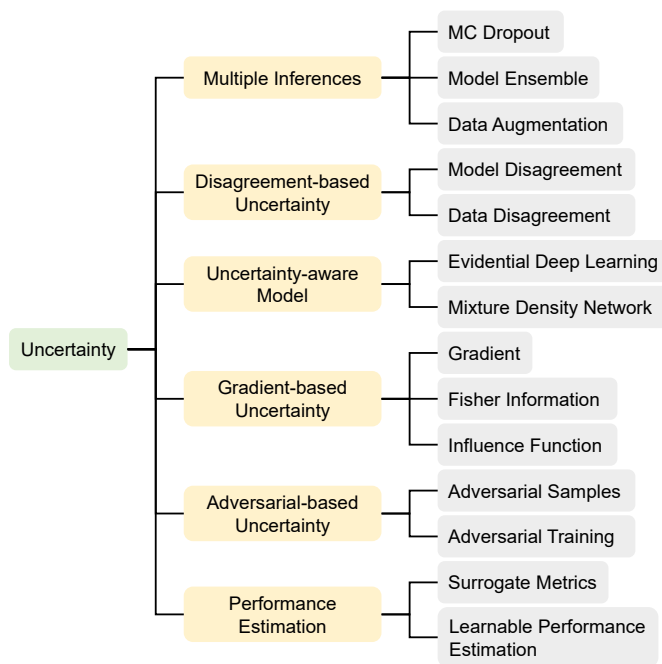


Figure 3: The taxonomy of uncertainty-based active learning.

MC dropout randomly discards some neurons in the deep model during each inference (Gal and Ghahramani, 2016). With MC dropout enabled, the model runs multiple times to get different predictions. Gal et al. (2017) was the pioneering work of deep AL. They were also the first to use MC dropout in computing uncertainty metrics like entropy, standard deviation, and Bayesian active learning disagreement (BALD) (Houlsby et al., 2011). Results showed that MC Dropout could significantly improve the performance of uncertainty-based deep AL.

Model ensemble trains multiple models to get numerous predictions during inference. Beluch et al. (2018) conducted a detailed comparison of models ensemble and MC dropout in uncertainty-based AL. Results demonstrated that the model ensemble performs better. However, model ensemble requires significant training overhead in DL. To reduce the computational costs, snapshot ensemble (Huang et al., 2017) obtained multiple models in a single run with cyclic learning rate decay. An early attempt in Beluch et al. (2018) showed that snapshot ensemble leads to worse performance than model ensemble. Jung et al. (2023) improved the snapshot ensemble by maintaining the same optimization trajectory in different AL rounds, along with parameter regularization. Results showed that the improved snapshot ensemble outperforms the model ensemble. Additionally, Nath et al. (2021) employed stein variational gradient descent to train an ensemble of models, aiming to ensure diversity among them.

Data augmentation produces different versions of input data with random transformations. Then, multiple predictions were obtained by running the model with different augmentations during inference. In point cloud semantic segmentation, Hu et al. (2022) randomly augmented the input point clouds

multiple times, then calculated the entropy of average prediction probability for each point after registration and correspondence estimation. Liu et al. (2022a) also applied random augmentations to point clouds, but they used variance as the uncertainty metric.

3.1.2. Disagreement-based Uncertainty

Disagreements between different inferences of the same sample could also be a measure of uncertainty. Samples with higher disagreement indicate higher uncertainty and are suitable for annotation. The principle of methods in this section aligns with the previous section, which aims to mitigate over-confidence by introducing perturbations during multiple inferences. However, methods in the previous section focus on improving the uncertainty estimation of classical metrics, while methods in this section leverage the disagreements between different prediction results. In this line of research, we can build disagreement from the perspective of model and data.

Model disagreement: We can utilize the disagreement between the outputs of different models, also known as Query-by-Committee (QBC) (Seung et al., 1992). Suggestive annotation (SA) (Yang et al., 2017) trained multiple segmentation networks with bootstrapping. The variance among these models is used as the disagreement metric. Mackowiak et al. (2018) adopted the vote entropy between different MC dropout inferences as the disagreement metric. Peng et al. (2021) trained teacher and student models through knowledge distillation and used the L2 distance of segmentation predictions as the disagreement metric. In polyp segmentation of capsule colonoscopy, Bai et al. (2022) trained multiple decoders using class activation maps (CAMs) (Zhou et al., 2016) generated by a classification network. They further proposed model disagreement and CAM disagreement for sample selection. Model disagreement included entropy of prediction probabilities and Dice between outputs of different decoders, while CAM disagreement measured the Dice between CAMs and outputs of all decoders. This method selected samples with high model disagreement and CAM disagreement for annotation. However, samples with low model disagreement but high CAM disagreement were treated as pseudo-labels for semi-supervised training. In rib fracture detection, Huang et al. (2020) adopted Hausdorff distance to measure the disagreements between different CAMs.

Data disagreement: Since training multiple models can be computationally expensive, measuring the disagreements between different perturbations of input data is also helpful in AL. Kullback-Leibler (KL) divergence is a commonly used metric for quantifying disagreement. Wu et al. (2021b) computed KL divergence between different versions of augmentations as the disagreement measure. Siddiqui et al. (2020) measured the disagreement with KL divergence between predictions of different viewpoints in 3D scenes. In point cloud segmentation, Hu et al. (2022) employed KL divergence to measure the disagreement between predictions of different frames. Additionally, recent works have adopted alternative metrics to calculate disagreement. Lyu et al. (2023) proposed

input-end committee, which constructs different predictions by randomly augmenting the input data. They further measured the classification and localization disagreements between different predictions with cross-entropy and variance, respectively. [Parvaneh et al. \(2022\)](#) interpolated the unlabeled samples and labeled prototypes in the feature space. If the prediction of the interpolated sample disagrees with the label of the prototype, it indicates that the unlabeled samples may introduce new features. Then, these unlabeled samples should be sent for annotation. Results showed advancements across various datasets and settings. Besides, some works explored the prediction disagreement within a local area inside an image. In object detection, [Aghdam et al. \(2019\)](#) assumed that the disagreement between probabilities in the neighborhood of wrongly predicted pixels should be high. They adopted BALD as the disagreement metric.

3.1.3. Uncertainty-aware Model

The main idea of uncertainty-aware models is to transform commonly used deterministic models into probabilistic models. In this way, the network no longer outputs a single point estimate but instead provides a distribution of possible predictions, thus mitigating over-confidence. This approach only requires a single pass of the deep model, significantly reducing computational and time costs during inference. Related works mainly fall into two categories: evidential deep learning (EDL) and mixture density networks (MDN).

Evidential deep learning replaces the Softmax distribution with a Dirichlet distribution ([Sensoy et al., 2018](#)). The network’s output is interpreted as the parameters of a Dirichlet distribution, so the predictions followed the Dirichlet distribution. The Dirichlet distribution will be sharp if the model is confident about the predictions. Otherwise, it will be flat. To make EDL compatible with object detection tasks, [Park et al. \(2023\)](#) introduced a model evidence head to scale the parameters of the Dirichlet distribution adaptively, which enhanced training stability. They first calculated the epistemic uncertainty for each detection box. Then, the sample-level uncertainty was obtained through hierarchical uncertainty aggregation. [Sun et al. \(2023\)](#) also applied EDL in scene graph generation, achieving near full-supervision performance with only about 10% of the labeling cost.

Mixture density networks: [Choi et al. \(2021a\)](#) transformed the classification and localization heads in object detection networks to the architecture of MDN ([Bishop, 1994](#)). Besides the coordinates and class predictions of each bounding box, the MDN heads produced the variance of classification and localization. They used the variances as uncertainty metrics for sample selection. Results showed that this method is competitive with MC dropout and model ensemble while significantly reducing the inference time and model size.

3.1.4. Gradient-based Uncertainty

Gradient-based optimization is essential for deep learning. The gradient of each sample reflects its contribution to the change of model parameters. A larger gradient length indicates a tremendous change of parameters by the sample, thus

implying high uncertainty. Furthermore, gradients are independent of predictive probabilities, making them less susceptible to over-confidence. In deep active learning, three metrics are frequently used as gradient-based uncertainty: gradients, Fisher information (FI), and influence functions.

Gradient: A larger gradient norm (i.e., gradient length) denotes a greater influence on model parameters, indicating higher uncertainty in AL. [Ash et al. \(2020\)](#) proposed batch active learning by diverse gradient embeddings (BADGE). They calculated the gradients only for the parameters of the network’s final layer, with the most confident classes as pseudo labels in gradient computation. Then, k-Means++ is performed on gradient embeddings for sample selection. Results showed competitive performances of BADGE across diverse datasets, network architectures, and hyperparameter settings. [Wang et al. \(2022b\)](#) proved that a larger gradient norm corresponds to a lower upper bound of test loss. Thus, they employed expected empirical loss and entropy loss for gradient computation, which both obviate the necessity for labels. The former was a sum of the losses for each class, which was weighted by the corresponding probability. The latter was the entropy of probabilities of all classes. In MRI brain tumor segmentation, [Dai et al. \(2020\)](#) employed gradients for active learning. They first trained a variational autoencoder (VAE) ([Kingma and Welling, 2013](#)) to learn the data manifold. Then, they trained a segmentation model and calculated gradients of Dice loss using available labeled data. The sample selection was guided by the gradient projected onto the data manifold. Their extended work ([Dai et al., 2022](#)) further demonstrated superior performance in MRI whole brain segmentation.

Fisher information: As the expectation of the gradient’s covariance matrix, FI reflects overall uncertainty according to the data distribution to model parameters. Annotating samples with higher FI helps the model converge faster toward optimal parameters. FI has already succeeded in AL of machine learning models ([Chaudhuri et al., 2015](#); [Sourati et al., 2017](#)). However, the computation cost of FI grows quadratically with the increase of model parameters, which is unacceptable for deep active learning. [Sourati et al. \(2018\)](#) and their extended work ([Sourati et al., 2019](#)) were the first to incorporate FI into deep active learning. They used the average gradients of each layer to calculate the FI matrix, thus reducing the computation cost. This method outperformed competitors in brain extraction across different age groups and pathological conditions. Additionally, [Ash et al. \(2021\)](#) only computed the FI matrix for the network’s last layer.

Influence functions: [Liu et al. \(2021b\)](#) employed influence functions ([Koh and Liang, 2017](#)) to select samples that bring the most positive impact on model performance. The method used expected empirical loss to calculate the gradient since influence functions also require gradient computations.

3.1.5. Adversarial-based Uncertainty

Uncertainty in AL can also be estimated adversarially, including adversarial samples and adversarial training.

Adversarial samples are created by adding carefully designed perturbations to normal samples by attacking the deep models

(Goodfellow et al., 2014b). The differences between adversarial and original samples are nearly indiscernible to the human eye. However, deep models would produce extremely confident wrong predictions for adversarial samples. The reason is that adversarial attacks push the original samples to the other side of the decision boundary with minimal cost, resulting in visually negligible changes but significantly different predictions. From this perspective, the strength of adversarial attacks reflects the sample’s distance to the decision boundary (Heo et al., 2019). A small perturbation indicates that the sample is closer to the decision boundary and, thus, is considered more uncertain. Ducoffe and Precioso (2018) adopted the DeepFool algorithm (Moosavi-Dezfooli et al., 2016) for adversarial attacks. Samples with small adversarial perturbations are requested for labeling. Rangwani et al. (2021) attacked the deep model by maximizing the KL divergence between predictions of adversarial and original samples while the strength of perturbation is limited.

Adversarial training involves alternating training between feature extractors and multiple classifiers. The objectives of training feature extractors and classifiers are conflicting. Multi-round adversarial training increases the disagreements between classifiers, uncovering uncertain samples hidden by over-confidence. In object detection, Yuan et al. (2021) and their extended work (Wan et al., 2023) used two classifiers for adversarial training on both labeled and unlabeled datasets. The first step is to fix the feature extractor and tune the two classifiers. The more classifiers disagreed the more uncertain samples were exposed. Then, they fixed the classifiers and tuned the feature extractor with opposite objectives, aiming to narrow the distribution gap between labeled and unlabeled samples. After multiple rounds of alternating training, samples with the highest disagreements between classifiers are sent for annotation. Fu et al. (2021) adversarially trained multiple classifiers to maximize their disagreement. The standard deviation between different predictions was considered the uncertainty metric.

3.1.6. Performance Estimation

In this section, the uncertainty metrics are direct performance estimations of the current task. There are two types of such metrics: test loss or task-specific evaluation metrics. These metrics reflect the level of prediction error. For instance, a low Dice score suggests the model failed to produce accurate segmentation. Request annotations for these samples would be beneficial for improving the model’s performance. However, instead of calculating these metrics precisely, we can only estimate them without the ground truths. There are primarily two methods for estimating performance: surrogate metrics and learnable performance estimation.

Surrogate metrics are widely used in this line of research. For example, these metrics may be upper or lower bounds for loss or some evaluation metrics. Huang et al. (2021) found that within limited training iterations, the loss of a sample is bounded by the norm of the difference between the initial and final network outputs. Inspired by this, they proposed cyclic output discrepancy (COD) as the difference in model output

between two consecutive annotation rounds. Results indicated that a higher COD is associated with higher loss. Therefore, they opted for samples with high COD. They may also demonstrate a linear correlation with the evaluation metrics with post-hoc validation. Shen et al. (2020) calculated the intersection over union (IoU) of all predictions by MC dropout. They found a strong linear correlation between this IoU and the real Dice coefficient. Zhao et al. (2021) calculated the average Dice coefficient between the predictions of the intermediate layers and final layer through deep supervision. They also found a linear correlation between this average Dice and the real Dice coefficient. Results showed competitive performance in skin lesion segmentation and X-ray hand bone segmentation.

Learnable performance estimation: Additionally, we can train auxiliary neural network modules to predict the performance metrics. As one of the most representative works in this line of research, learning loss for active learning (LL4AL) (Yoo and Kweon, 2019) trained an additional module to predict the loss value of a sample without its label. Since loss indicates the quality of network predictions, the predicted loss is a natural uncertainty metric for sample selection. Results showed that predicted and actual losses are strongly correlated. LL4AL also outperformed several AL baselines. In lung nodule detection with CT scans, Liu et al. (2020) built upon LL4AL to predict the loss of each sample and bounding box. In diagnosing COVID-19, Wu et al. (2021b) adopted both the predicted loss and the disagreements between different predictions for sample selection. Since AL focuses only on uncertainty ranking of the unlabeled samples, Kim et al. (2021) relaxed the loss regression to loss ranking prediction. Thus, they replaced the loss regressor in LL4AL with the ranker in RankCGAN (Saqil et al., 2018). Results showed that loss ranking prediction outperforms LL4AL.

3.2. Evaluation of Informativeness: Representativeness

While uncertainty methods play a crucial role in deep AL, they still face certain challenges: **1. Outlier selection:** The goal of using uncertainty in AL is to improve performance by querying hard samples of the current model. However, these methods could also select outliers that harm the model training (Karamcheti et al., 2021). This happens because uncertainty relies solely on model predictions and ignores the exploration of intrinsic characteristics of the data distribution. Incorporating an additional informativeness measure to remove outliers would be beneficial for AL. **2. Distribution misalignment:** Samples selected by uncertainty methods are often located near the decision boundary in the feature space (Settles, 2009). Therefore, the distribution of selected samples by uncertainty-based method may differ from the overall data distribution. This discrepancy may introduce dataset bias and lead to a performance drop. Therefore, the challenges above compel us further to discover the data distribution during the evaluation of informativeness.

Representativeness-based deep AL aims to select a subset of samples that can represent the entire dataset. Generally, highly representative samples are located in dense regions of the data manifold and contain information about other nearby

samples. Moreover, these methods require diversity in sampling result. Representative samples should be widely distributed across the data manifold rather than concentrated in a specific region. Besides, representative samples should be visually distinctive in properties like imaging style or visual content. Deep feature representations encode such information and are used to calculate the mutual relationships between different samples. This section introduces three formulations of representativeness-based AL: cover-based, discrepancy-based, and density-based representativeness AL. The taxonomy of these methods is shown in Fig. 4.

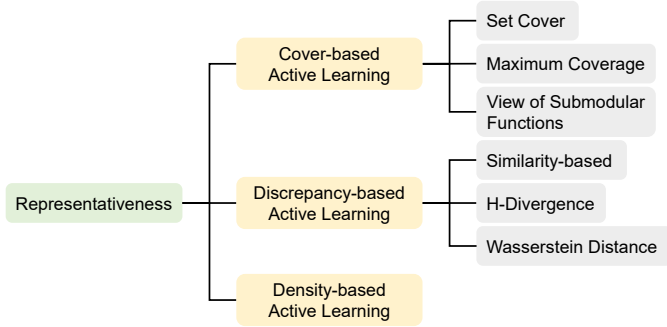


Figure 4: The taxonomy of representativeness-based active learning.

3.2.1. Cover-based Active Learning

We can formulate representativeness-based AL as a problem of covering. A classic example of the covering problem is the facility location, such as covering all the city’s streets with some billboards (Farahani and Hekmatfar, 2009). Likewise, cover-based AL uses a few samples to cover the entire dataset. Ideally, these samples should be representative and contain information from other samples. These methods usually involve two settings: set cover and maximum coverage. Both settings are NP-hard, meaning they cannot be optimally solved in polynomial time. However, near-optimal solutions could be achieved in linear time using greedy algorithms. Specifically, the greedy algorithms iteratively select samples that cover other samples the most for annotation (Feige, 1998).

Set cover aims to select as few samples as possible to cover the entire dataset. CoreSet (Sener and Savarese, 2018) followed the setting of k-Center location (Hochbaum and Shmoys, 1985), which is also a variant of the set cover problem. In CoreSet, the L2 distance of deep features measures the similarity between different samples. They employed farthest-first traversal to solve the k-Center problem for selecting representative samples. Agarwal et al. (2020) introduced contextual diversity for AL, a metric that fused uncertainty and diversity of samples spatially and semantically. They replaced the L2 distance with contextual diversity and used the same method in CoreSet for sample selection. Caramalau et al. (2021) adopted graph convolutional networks (GCN) to model the relationships between labeled and unlabeled samples. GCNs improved the feature representation of unlabeled samples with the labeled dataset. Enhanced feature representation was further used for CoreSet sampling.

Maximum coverage selects a given number of samples to cover the entire dataset as much as possible. Yehuda et al. (2022) found that CoreSet tends to select outliers, especially when the annotation budget is low. To address this issue, they proposed ProbCover, which changed the setting from set cover to maximum coverage. They employed a graph-based greedy algorithm for sample selection. With the help of self-supervised deep features, ProbCover effectively avoided selecting outlier samples. Additionally, SA (Yang et al., 2017) provides another formulation of maximum coverage. SA first selected highly uncertain samples and then further chose representative samples for annotation. The representativeness was based on the cosine similarity of deep features. Specifically, sample x is represented by the most similar sample from queried dataset D_t^q

$$r(D_t^q, x) = \max_{x' \in D_t^q} \text{sim}(x', x) \quad (5)$$

where r is the representativeness of sample x with respect to D_t^q and $\text{sim}(\cdot, \cdot)$ represents cosine similarity. Besides, representativeness R between D_t^q and the unlabeled set D_t^u is as follow:

$$R(D_t^q, D_t^u) = \sum_{x \in D_t^u} r(D_t^q, x) \quad (6)$$

where a larger $R(D_t^q, D_t^u)$ indicates that D_t^q better represents D_t^u . It should be noted that SA is a generalization of the maximum coverage problem since the cosine similarity ranges from 0 to 1. But they still employed a greedy algorithm to find sample x that maximizing $R(D_t^q \cup x, D_t^u) - R(D_t^q, D_t^u)$. SA has inspired many subsequent works. Xu et al. (2018) quantized the segmentation networks in SA and found that it improved the accuracy of gland segmentation while significantly reducing memory usage. Zheng et al. (2019) proposed representative annotation (RA), which omits the uncertainty query in SA. RA trained a VAE for feature extraction and partitioned the feature space using hierarchical clustering. They selected representative samples in each cluster using a similar strategy to SA. Shen et al. (2020) changed the similarity measure in SA from $\text{sim}(\cdot, \cdot)$ to $1 - \text{sim}(\cdot, \cdot)$, which enhanced the diversity of the selected samples. In keypoint detection of medical images, Quan et al. (2022) proposed a representative method to select template images for few-shot learning. First, they trained a feature extractor using self-supervised learning and applied SIFT for initial keypoint detection. Next, they calculated the average cosine similarity between template images and the entire dataset. Finally, they picked the template combination with the highest similarity for annotation.

View of submodular functions: Both set cover and maximum coverage can be formulated from the perspective of submodular functions (Fujishige, 2005). These functions show diminishing marginal returns, meaning each added element brings less gain than the previous one as the set gets larger. Generally, each submodular function corresponds to a particular optimization problem. If a submodular function is

monotonic and non-negative, we can use a greedy algorithm to get near-optimal solutions in linear time. In cover-based AL, methods like SA and RA followed the setting of submodular functions, but the authors didn't present their methods from this perspective. Introducing submodular functions would extend the formulation of AL and ensure the selected samples are both representative and diverse. Typical steps for this type of method involve calculating sample similarities, constructing a submodular optimization problem, and solving it using a greedy algorithm (Wei et al., 2015). Kothawade et al. (2021) introduced an AL framework based on submodular information measures, effectively addressing issues such as scarcity of rare class, redundancy, and out-of-distribution data. In object detection, Kothawade et al. (2022a) focused on samples of minority classes. They constructed a set of classes of interest and selected unlabeled samples similar to these classes for annotation through submodular mutual information (Kothawade et al., 2022b).

3.2.2. Discrepancy-based Active Learning

In discrepancy-based AL, unlabeled samples farthest from the labeled set are considered the most representative. The main idea is that if we queried such samples for multiple rounds, the discrepancy between the distributions of labeled and unlabeled sets would be significantly reduced. Therefore, a small set of samples could well represent the entire dataset. The key to these methods is measuring the discrepancy (i.e., distance) between two high-dimensional distributions. This section presents three metrics for measuring discrepancy: similarity-based discrepancy, H-divergence, and Wasserstein distance.

Similarity-based discrepancy: As a practical and easy-to-implement metric, we can approximate the distance between distributions based on sample similarity. Caramalau et al. (2021) proposed UncertainGCN, which employed GCN to model the relationship between labeled and unlabeled samples. They selected the unlabeled samples with the lowest similarity to the labeled set. In gland and MRI infant brain segmentation, Li and Yin (2020) adopted the average cosine similarity as the distance between two datasets. They selected samples far from the labeled set and close to the unlabeled set. In object detection, Wu et al. (2022a) constructed prototypes with sample features and prediction entropy. They selected unlabeled samples that were far from the labeled prototype.

H-divergence estimates the distance of distribution with the help of the discriminator from generative adversarial networks (GAN) (Goodfellow et al., 2014a). More specifically, the discriminator tries to distinguish between labeled and unlabeled samples, and there is a close relationship between H-divergence and the discriminator's output (Gissin and Shalev-Shwartz, 2019). Variational adversarial active learning (VAAL) (Sinha et al., 2019) combined VAE with a discriminator for discrepancy-based AL. In VAAL, the VAE mapped samples to a latent space while the discriminator distinguished whether samples were labeled. These two are mutually influenced by adversarial training. VAE tried to fool the discriminator into judging all samples as labeled while the

discriminator attempted to correctly differentiate between labeled and unlabeled samples. After multiple rounds of adversarial training, VAAL selected samples that the discriminator deemed most likely to be unlabeled for annotation. Unlike VAAL, Gissin and Shalev-Shwartz (2019) trained the discriminator without adversarial training. Zhang et al. (2020) replaced the discriminator's binary label with sample uncertainty. They also combined features of VAE with features from the supervised model. Wang et al. (2020b) adopted a neural network module for sample selection. To train such a module, they added another discriminator on top of VAAL, which aimed to differentiate between the real and VAE-reconstructed features for unlabeled samples. After adversarial training of both discriminators, the module selected uncertain and representative samples. Kim et al. (2021) combined LL4AL with VAAL, feeding both loss ranking predictions and VAE features into the discriminator.

Wasserstein distance is widely used for computing distribution distances. Shui et al. (2020) indicated that H-divergence may compromise the diversity of sample selection, while Wasserstein distance ensures the queried samples are representative and diverse. They further proposed Wasserstein adversarial active learning (WAAL). Specifically, WAAL was built upon VAAL and adopted an additional module for sample selection. They trained this module by minimizing the Wasserstein distance between labeled and unlabeled sets. WAAL selected samples that are highly uncertain and most likely to be unlabeled for annotation. Mahmood et al. (2022) formulated AL as an optimal transport problem. They aimed at minimizing the Wasserstein distance between the labeled and unlabeled sets with self-supervised features. They further adopted mixed-integer programming that guarantees global convergence for diverse sample selection. Moreover, Xie et al. (2023b) considered the candidates as continuously optimizable variables based on self-supervised features. They randomly initialized the candidate samples at first. Then, they maximized the similarity between candidates and their nearest neighbors while minimizing the similarity between candidates and labeled samples. Finally, they selected the nearest neighbors of the final candidates for annotation. They proved the objective is equivalent to minimizing the Wasserstein distance between the labeled and unlabeled samples.

3.2.3. Density-based Active Learning

Density-based AL employs density estimation to characterize the data distribution in a high-dimensional feature space. The likelihood is the estimated density of the data distribution, and a more densely populated area indicates a higher likelihood. In this case, representative samples are samples with high likelihood. However, such methods can easily cause redundancy in sample selection. As a result, techniques like clustering are frequently used to improve diversity in sample selection. Density-based AL directly estimates the data distribution, which prevents the need to solve complex optimization problems. TypiClust (Hacohen et al., 2022) projected samples to a high-dimensional feature space via a self-supervised encoder. The density of a sample was defined as the reciprocal

of the L2 distances to its k-nearest neighbors. Additionally, TypiClust performed clustering beforehand to ensure the diversity of selected samples. Wang et al. (2022c) proposed two variants of density-based AL. The first variant fixed the feature representation. The process was similar to TypiClust, but they maximized the distances between selected samples to ensure diversity. The other variant was in an end-to-end fashion. Feature representation and sample selection were trained simultaneously. This variant used a learnable k-Means clustering to jointly optimize cluster assignment and feature representation with a local smoothness constraint.

In active domain adaptation, density estimation is also widely used to select representative samples in the target domain. Please refer to §4.3 for related works.

3.3. Sampling Strategy

Most deep AL works used top-k to select samples with the highest informativeness for annotation. However, existing informativeness metrics face several issues, such as redundancy and class imbalance in selected samples. Instead of improving informativeness, we can introduce simple sampling strategies to resolve these issues effectively. Besides, specific sampling strategies can also be used for combining multiple informativeness metrics. Furthermore, with the recent development of deep AL, more studies directly employ neural networks for sample selection. In this context, we no longer evaluate informativeness but directly choose valuable samples from the unlabeled pool with neural networks. In summary, sampling strategies are crucial in AL, but prior surveys have seldom discussed their specific attributes. As one of the contributions of this survey, we systematically summarize different sampling strategies in AL, including diversity sampling, class-balanced sampling, hybrid sampling, and learnable sampling. The taxonomy of different sampling strategies in AL is shown in Fig. 5.

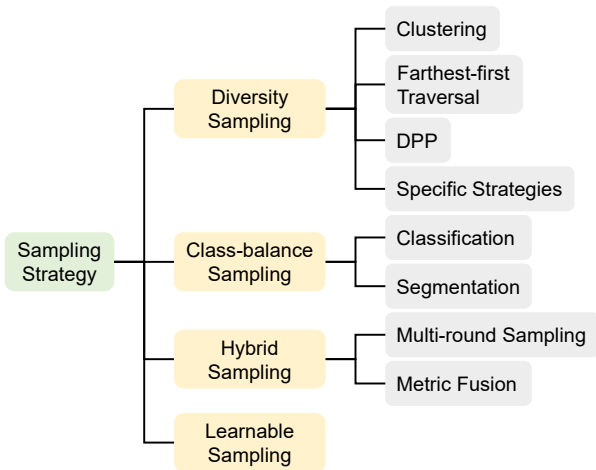


Figure 5: The taxonomy of different sampling strategies in active learning.

3.3.1. Diversity Sampling

Diversity strategies aim to reduce redundancy in selected samples. Sampling redundancy is a common issue for

uncertainty-based and representativeness-based methods, meaning some selected samples are highly similar. The lack of diversity leads to the waste of the annotation budget. Besides, redundancy in the training set may cause deep models to overfit, thus degrading performance. Therefore, many AL methods employ diversity sampling to mitigate the redundancy in selected samples. In this section, we discuss four strategies of diversity sampling, including clustering, farthest-first traversal, determinantal point process (DPP), and specific strategies tailored to certain informativeness metrics.

Clustering is one of the most commonly used strategies of diversity sampling. It groups the data into several clusters and then queries samples within each cluster. This strategy improves the coverage of the entire feature space, thereby easily boosting diversity. Ash et al. (2020) employed k-Means++ clustering on gradient embeddings to select diverse uncertain samples. Citovsky et al. (2021) boosted margin-based uncertainty sampling with hierarchical clustering. They selected samples with the smallest margins within each cluster. When the number of queries exceeded the number of clusters, samples from smaller clusters were prioritized. This method can extend to a huge annotation budget (e.g., one million). Jin et al. (2022a) employed BIRCH clustering and chose the samples with maximum information density within each cluster for labeling. Compared to k-Means, BIRCH clustering is less sensitive to outliers and can further identify noisy samples. In connectomics, Lin et al. (2020) trained two feature extractors with labeled and unlabeled samples, respectively. They then selected samples for annotation through multiple rounds of clustering. This method achieved excellent performance in synapse detection and mitochondria segmentation.

Farthest-first Traversal is also a widely used strategy for diverse queries. The farthest-first traversal requires the distance between sampling points to be as large as possible in the feature space. This leads to a more uniform distribution of selected samples within the feature space, thus improving the diversity of the sampling results. This technique was first adopted by Sener and Savarese (2018). Agarwal et al. (2020) and Caramalau et al. (2021) improved the diversity with farthest-first traversal, leveraging their proposed contextual diversity and GNN-augmented features, respectively. However, when the annotation budget is limited, the farthest-first traversal may be biased toward outliers.

Determinantal point process is a stochastic probability model for selecting subsets from a larger set. DPP reduces the probability of sampling similar elements to ensure diversity in the results. Bıyık et al. (2019) employed two DPPs for sample selection: Uncertainty DPP is based on uncertainty scores, while Exploration DPP aims to find samples near decision boundaries. Then, sampling results from both DPPs were sent for expert annotation. However, DPP is more computationally intensive compared to clustering. Ash et al. (2020) compared the performance and time cost of using k-Means++ and k-DPP. Results showed that their performance is similar, but the time cost for k-Means++ is significantly lower than that for k-DPP.

Specific strategies: There are also specific strategies tailored to certain informativeness metrics. In uncertainty-based AL,

BatchBALD (Kirsch et al., 2019) extended BALD-based uncertainty AL to batch mode. Results showed that BatchBALD improved the sampling diversity compared to (Gal et al., 2017). FI-based methods formulated AL as a semi-definite programming (SDP) problem to improve sampling diversity. Different methods were employed for solving SDP. Sourati et al. (2019) used a commercial solver to solve SDP, while Ash et al. (2021) proposed a greedy algorithm to adapt to high-dimensional feature space. Moreover, diversity is an essential part of representativeness-based AL. Cover-based AL inherently incorporates the considerations of diversity in its formulations. In discrepancy-based AL, Wasserstein distance is used for diverse query results (Shui et al., 2020; Mahmood et al., 2022). Density-based methods often employ strategies like clustering to improve diversity.

3.3.2. Class-balance Sampling

Class imbalance is a common issue for DL, where a small set of classes have many samples while the others only contain a few samples (Zhang et al., 2023). For example, in tasks such as medical image classification, normal samples often outnumber abnormal ones. Training on imbalanced datasets can lead to the overfitting of the majority classes and underfitting of the minority classes. Apart from dealing with class imbalance during training, AL mitigates class imbalance by avoiding over-annotation of the majority classes and enhancing the annotation of the minority classes during dataset construction. **Classification:** Choi et al. (2021b) directly estimated the probability of a classifier making a mistake for a given sample and decomposed it into three terms using Bayesian rules. First, they trained a VAE to estimate the likelihood of the data given a predicted class. Then, an additional classifier was trained upon VAE features to estimate class prior probabilities and the probability of mislabeling a specific class. By considering all three probabilities, they successfully mitigated class imbalance in AL. The proposed method achieved good performance on stepwise class-imbalanced CIFAR-10 and CIFAR-100 datasets. For uncertainty-based methods, Bengar et al. (2022) introduced an optimization framework to maintain class balance. They compensated the query of minority classes with the most confident samples of that class, leading to a more balanced class distribution in the queried dataset. In classification tasks, Munjal et al. (2022) tested various AL baselines on the long-tailed CIFAR-100 dataset. Results showed that no single method outperforms others on all budgets in the class-imbalance setting. However, as the number of labeled data increases, the performance gap between random sampling and the best AL method decreases. Hacohen et al. (2022) conducted experiments in a class-imbalanced setting similar to Munjal et al. (2022). The proposed TypiClust ensured class balance and outperformed other baseline methods. Jin et al. (2022c) assumed that samples closer to the tail of the distribution are more likely to belong to the minority classes. Thus, the tail probability is equivalent to the likelihood of minority classes. Specifically, they trained a VAE for feature extraction and adopted copula to estimate the tail probabilities upon VAE features. Finally, informative samples were selected

with clustering and unequal probability sampling. The proposed method was validated on the ISIC 2020 dataset, which has a long-tailed distribution. Kothawade et al. (2022c) used submodular mutual information to focus more on samples of minority classes. They achieved excellent results on medical classification datasets in five different modalities, including X-rays, pathology, and dermoscopy. Besides, in blood cell detection under microscopy, Sadafi et al. (2019) requested expert annotation of a sample whenever its classification probability of the minority class exceeded 0.2.

Segmentation: Due to some AL methods selecting regions instead of the entire image for annotation, there is a need to ensure that the selected regions contain rare or small objects (e.g., pedestrians or utility poles in autonomous driving). Cai et al. (2021) and Wu et al. (2022b) both proposed class-balanced sampling strategies for such scenarios, as detailed in §4.4.

3.3.3. Hybrid Sampling

In AL, some works may use multiple informativeness metrics simultaneously. Therefore, the effective integration of multiple metrics remains a critical issue. This issue is addressed by the hybrid sampling strategy discussed in this section. Two approaches to hybrid sampling are primarily used, including multi-round sampling and metric fusion.

Multi-round sampling first selects a subset of samples based on one particular informativeness metric and continues sample selection within this subset based on another informativeness metric. For example, SA (Yang et al., 2017) performed representativeness sampling based on uncertainty to reduce redundancy in the sampled set. Xie et al. (2022b) first selected samples with density-based methods and selected the most uncertain samples within each cluster of representative samples. In another study, Xie et al. (2022c) introduced distribution and data uncertainty based on EDL, and then a two-stage strategy was used for sample selection. Wu et al. (2022b) employed a more complex strategy, which sets dynamic weights to adjust the budget of representativeness and uncertainty sampling. The weight of representativeness sampling is larger initially, while the situation is reversed in the latter phase. This is because representativeness methods can quickly spot typical data, while uncertainty methods continuously improve the model by querying samples with erroneous predictions.

Metric fusion is another widely used approach of hybrid sampling. It directly combines different informativeness metrics. For example, one could directly sum up all metrics and select the samples with the highest values for annotation. Ranked batch-mode (Cardoso et al., 2017) can adaptively fuse multiple metrics in AL.

3.3.4. Learnable Sampling

Previously mentioned AL methods typically follow a “two-step” paradigm, which first involves the evaluation of informativeness and then selects samples based on specific heuristics (i.e., sampling strategy). However, learnable sampling skips the informativeness evaluation and directly

uses neural networks for sample selection. In this context, the neural network is known as a “neural selector”.

One of the most common methods of learnable sampling is to formulate sample selection as a reinforcement learning (RL) problem, where the learner and the dataset are considered the environment, and the neural selector serves as the agent. The agent interacts with the environment by selecting a limited number of samples for annotation, and the environment returns a reward to train the neural selector. [Haußmann et al. \(2019\)](#) adopted a probabilistic policy network as the neural selector. The rewards returned by the environment encouraged the neural selector to choose diverse and representative samples. The neural selector is trained using the REINFORCE algorithm ([Williams, 1992](#)). In pedestrian re-identification, [Liu et al. \(2019\)](#) used the annotation uncertainty as the reward for training the neural selector. [Agarwal et al. \(2020\)](#) utilized the proposed contextual diversity as RL rewards and trains a bidirectional long short-term memory network as the neural selector. In pose estimation, [Gong et al. \(2022\)](#) adopted multiple agents for sample selection and directly used the performance improvement of the pose estimator as the reward for training these agents. In medical image classification, [Wang et al. \(2020a\)](#) employed an actor-critic framework where the critic network is used to evaluate the quality of the samples selected by the neural selector. This method has performed excellently in lung CT disease classification and diabetic retinopathy classification of fundus images.

For more works on learnable sampling in AL, such as formulating AL as few-shot learning or training neural selectors by meta-learning, please refer to the survey of [Liu et al. \(2022b\)](#).

4. Integration of Active Learning and Other Label-Efficient Techniques

Various methods have been proposed to reduce the large amount of labeled data required for training deep models, such as active learning, semi-supervised learning, self-supervised learning, etc. These methods are collectively called label-efficient deep learning ([Jin et al., 2023a](#)). Label-efficient learning is a broad concept that includes all related technologies designed to improve annotation efficiency. In §3, we summarized the core methods in AL, including the evaluation of informativeness and sampling strategies. However, there is still room for AL to further improve the label efficiency. For example, AL has not used unlabeled data for training, has not considered distribution shift, and still needs to annotate the whole image in fine-grained tasks such as segmentation. Integrating active learning with other label-efficient techniques can increase annotation efficiency. While some efforts have been made, existing surveys have not yet systematically organized and categorized this line of work. Hence, as one of the main contributions of this survey, we comprehensively reviewed the integration of AL with other label-efficient techniques, including semi-supervised learning, self-supervised learning, domain adaptation, region-based annotation, and generative

models. Additionally, how each surveyed work integrated with other label-efficient techniques is summarized in Table 2.

4.1. Semi-supervised Learning: Utilizing Unlabeled Data

Semi-supervised learning ([Chen et al., 2022a](#)) aims to boost performance by utilizing unlabeled data upon supervised training. AL and semi-supervised learning complements each other: AL focuses on constructing an optimal labeled dataset. However, massive unlabeled samples are discarded during model training. Therefore, we can further leverage unlabeled data to train the deep model. By integrating the strengths of both AL and semi-supervised learning, annotation efficiency can be further improved. This section will introduce the integration of AL and semi-supervised learning from pseudo-labeling and consistency regularization.

4.1.1. Pseudo-Labeling

Pseudo-labeling ([Lee et al., 2013](#)) is one of the most straightforward methods in semi-supervised learning. It uses the model’s predictions of unlabeled data as pseudo-labels and combines them with labeled data for supervised training. Although it’s possible to assign pseudo-labels to all unlabeled samples for training, it may introduce noise. To mitigate this, [Wang et al. \(2017\)](#) proposed cost-effective active learning (CEAL), integrating pseudo-labeling with uncertainty-based AL. Specifically, CEAL sent the most uncertain samples for expert annotation and assigned pseudo-labels to the most confident samples. Many subsequent works have built upon the ideas of CEAL. In point cloud segmentation, both [Hu et al. \(2022\)](#) and [Liu et al. \(2022a\)](#) assigned pseudo-labels of the most certain regions. In medical image segmentation, [Zhao et al. \(2021\)](#) refined the pseudo-labels with dense conditional random fields. Additionally, [Li et al. \(2022\)](#) proposed a new approach for selecting samples for oracle annotation and pseudo-label. Specifically, they employed curriculum learning to categorize all samples into hard and easy. Hard samples were all sent for oracle annotation. For the easy samples, they evaluated the presence of label noise based on the training loss. Easy samples with low training loss were used for pseudo-labels to assist training, whereas easy samples with high loss were considered noisy and excluded from training.

4.1.2. Consistency Regularization

Consistency regularization is also widely applied in semi-supervised learning. Its basic idea is to enforce consistent outputs under perturbations of input data or model parameters. Maximizing consistency serves as an unsupervised loss for unlabeled samples. Consistency regularization helps improve the robustness and reduce overfitting of the model, thus enhancing model performance. [Gao et al. \(2020\)](#) introduced a semi-supervised active learning framework. Consistency here was used for both semi-supervised training and evaluating informativeness. In this framework, samples are fed into the model multiple times with random augmentations. The consistency loss of unlabeled samples was implemented by minimizing the variance between multiple outputs. They

Table 2: Methodology summarization of surveyed active learning works.

Year	Venues	Uncertainty		Representativeness			Sampling Strategy	SemiSL	SelfSL	ADA	Region	Generative
		Method	Method	Basic Metrics	Method	Basic Metrics						
Zhu and Bento (2017)	2017	arXiv	Single Model	Distance to Decision Boundary	-	-	Top-k					✓
Zhou et al. (2017)	2017	CVPR	Single Model Data Disagreement	Entropy KL Divergence	-	-	Hybrid - Fusion					
Gal et al. (2017)	2017	ICML	Multiple Inferences - MC Dropout	Entropy, BALD, Least Confidence, Variance	-	-	Top-k					
Yang et al. (2017)	2017	MICCAI	Model Disagreement	Variance	Cover-based	Cosine Similarity	Hybrid - Multi-round			Pseudo-label		
Wang et al. (2017)	2017	TCSVT	Single Model	Least Confidence, Margin, Entropy	-	-	Top-k					
Ducicco and Precioso (2018)	2018	arXiv	Adversarial Samples	Distance to Decision Boundary	-	-	Top-k					
Mackowiak et al. (2018)	2018	BMVC	Model Disagreement	Vote Entropy	-	-	Top-k					Patch
Xu et al. (2018)	2018	CVPR	Multiple Inferences - Model Ensemble	Variance	Cover-based	Cosine Similarity	Hybrid - Multi-round					
Beluch et al. (2018)	2018	CVPR	Multiple Inferences - Model Ensemble	Entropy, BALD, Least Confidence, Variance	-	-	Top-k					
Sourati et al. (2018)	2018	DLMIA	Gradient-based Metrics	Fisher Information	-	-	Diversity - Solve Programming Problem					
Sener and Savarese (2018)	2018	ICLR	-	-	Cover-based	L2 Distance	Diversity - Farthest-first Traversal					
Kuo et al. (2018)	2018	MICCAI	Model Disagreement	JS Divergence	-	-	Diversity - Solve Programming Problem					
Mahapatra et al. (2018)	2018	MICCAI	Multiple Inferences - MC Dropout	Variance	-	-	Top-k					✓
Haußmann et al. (2019)	2019	IJCAI	-	-	-	-	Learnable - Reinforcement Learning					
Zheng et al. (2019)	2019	AAAI	-	-	Cover-based	Cosine Similarity	Diversity - Clustering			✓		
Gissin and Shalev-Shwartz (2019)	2019	arXiv	-	-	Discrepancy-based	H-Divergence	Top-k					
Yoo and Kweon (2019)	2019	CVPR	Performance Estimation - Learnable	Loss	-	-	Top-k					
Sinha et al. (2019)	2019	ICCV	-	-	Discrepancy-based	H-Divergence	Top-k					
Liu et al. (2019)	2019	ICCV	-	-	-	-	Learnable - Reinforcement Learning					
Aghdam et al. (2019)	2019	ICCV	Data Disagreement	BALD	-	-	Top-K					
Tran et al. (2019)	2019	ICML	Multiple Inferences - MC Dropout	BALD	-	-	Top-k					✓
Qi et al. (2019)	2019	JBHI	Single Model	Entropy	-	-	Top-k			Pseudo-label		
Sudafi et al. (2019)	2019	MICCAI	Multiple Inferences - MC Dropout	Average IoU, Class Frequency	-	-	Class-balance Hybrid - Fusion					
Kirsch et al. (2019)	2019	NeurIPS	Multiple Inferences - MC Dropout	BALD	-	-	Top-k					
Sourati et al. (2019)	2019	TMI	Gradient-based Metrics	Fisher Information	-	-	Diversity - Solve Programming Problem					
Kasaria et al. (2019)	2019	WACV	Single Model	Entropy	-	-	Top-k					Superpixel
Zheng et al. (2020)	2020	AAAI	-	-	Cover-based	Cosine Similarity	Diversity - Clustering			Pseudo-label		Slice
Shui et al. (2020)	2020	AISTATS	Single Model	Entropy, Least Confidence	Discrepancy-based	Wasserstein Distance	Hybrid - Fusion					✓
Siddiqui et al. (2020)	2020	CVPR	Multiple Inferences - MC Dropout	Entropy KL Divergence	-	-	Hybrid - Fusion					Superpixel
Zhang et al. (2020)	2020	CVPR	Single Model	Variance	Discrepancy-based	H-Divergence	Diversity - Farthest-first Traversal					
Gao et al. (2020)	2020	ECCV	Data Disagreement	Variance	-	-	Top-k			Consistency		
Wang et al. (2020b)	2020	ECCV	-	-	Discrepancy-based	H-Divergence	Learnable					
Agarwal et al. (2020)	2020	ECCV	-	-	Cover-based	Contextual Diversity	Diversity - Farthest-first Traversal Learnable - Reinforcement Learning					
Lin et al. (2020)	2020	ECCV	-	-	Clustering	L2 Distance	Diversity - Clustering					
Ash et al. (2020)	2020	ICLR	Gradient-based Metrics	Gradient	-	-	Diversity - Clustering					
Casanova et al. (2020)	2020	ICLR	-	-	-	-	Learnable - Reinforcement Learning					Patch
Dai et al. (2020)	2020	MICCAI	Gradient-based Metrics	Gradient	-	-	Latent Space Optimization & Nearest Neighbour Search					Slice

Table 2: Methodology summarization of surveyed active learning works.

Year	Vvenues	Uncertainty		Representativeness		SemiSL	SelfSL	ADA	Region	Generative
		Method	Basic Metrics	Method	Basic Metrics					
2020	MICCAI	Multiple Inferences - MC Dropout	Entropy	Cover-based	Cosine Similarity				Hybrid - Multi-round	
		Performance Estimation - Surrogate	IoU of all result							
2020	MICCAI	Performance Estimation - Learnable	Loss	-	-				Top-k	
2020	MICCAI	Multiple Inferences - Model Ensemble	Margin	Discrepancy-based	Cosine Similarity				Hybrid - Multi-round	
2020	MICCAI	-	-	-	-				Learnable - Reinforcement Learning	
2020	MICCAI	-	-	-	-				Hybrid - Multi-round	Slice, Pixel
2020	TMI	Multiple Inferences - MC Dropout	Variance	Cover-based	Cosine Similarity				Top-k	
2020	TMI	Model Disagreement	Hausdorff Distance	-	-					
2020	WACV	Single Model	Entropy	Discrepancy-based	H-Divergence				Hybrid - Fusion	✓
2021	CVPR	Probability of Misclassification	-	-	-				Class-balance	
2021	CVPR	Adversarial Training	Disagreement of Classifiers, margin	Discrepancy-based	H-Divergence				Hybrid - Fusion	✓
2021	CVPR	-	-	Clustering	L2 Distance				Diversity - Clustering	✓
2021	CVPR	Performance Estimation - Learnable	Rank of Loss	Discrepancy-based	H-Divergence				Top-k	
2021	CVPR	Adversarial Training	Disagreement of Classifiers	-	-				Top-k	
2021	CVPR	Single Model	BvSB	-	-				Class-balance	Superpixel
2021	CVPR	Single Model (w/ GNN)	Margin	Cover-based	L2 Distance of GCN-augmented Features				Top-k	
2021	ICCV	Single Model	Entropy	-	-				Diversity - Farthest-first Traversal	
2021	ICCV	-	-	Discrepancy-based	L2 Distance				Diversity - Clustering	✓
2021	ICCV	Performance Estimation - Surrogate	Temporal Output Discrepancy	-	-				Diversity - Clustering	
2021	ICCV	-	-	Discrepancy-based	Semantic and distinctive scores				Top-k	Consistency
2021	ICCV	Model Disagreement	Inequality	-	-				Hybrid - Fusion	✓
2021	ICCV	Single Model	Entropy	Clustering	Color-Difference Surface Variation				Diversity - Clustering	Pseudo-label
2021	ICCV	Adversarial Samples	KL Divergence	Cover-based - Submodular	KL Divergence Bhattacharyya Coefficient				Hybrid - Fusion	Superpixel
2021	ICCV	Uncertainty-aware Models - MDN	Variance	-	-				Hybrid - Fusion	✓
2021	ICCV	Model Disagreement	L2 Distance	Cover-based	Cardinal of Difference Set				Top-k	
2021	ICCV	Gradient-based Metrics	Influence	-	-				Hybrid - Fusion	
2021	JBHI	Performance Estimation - Surrogate	Dice	-	-				Top-k	Pseudo-label
2021	Media	Single Model	Entropy	-	-				Top-k	
2021	Media	Data Disagreement	KL Divergence	-	-				Hybrid - Fusion	
2021	Media	Performance Estimation - Learnable	Loss	-	-				Hybrid - Fusion	
2021	MICCAI	Performance Estimation - Learnable	Dice	-	-				Top-k	
2021	MICCAI	Single Model	Distance to Mean Probability	-	-				Top-k	Consistency
2021	MICCAI	Multiple Inferences - Model Ensemble	Variance	Discrepancy-based	Cosine Similarity				Top-k	Consistency
2021	MIDL	Single Model	Entropy	Cover-based	L2 Distance				Diversity - Clustering	Consistency
2021	NeurIPS	Gradient-based Metrics	Fisher Information	-	-				Hybrid - Multi-round	
2021	NeurIPS	-	-	Cover-based - Submodular	Gradient				Diversity - Clustering	Pseudo-label
2021	NeurIPS	Single Model	Margin	-	-				Diversity - Solve Programming Problem	✓
2021	TMI	Multiple Inferences - Model Ensemble	Entropy	Discrepancy-based	Mutual Information				Top-k	
2021	TMI	-	-	Saliency Maps	Kurtosis				Diversity - Clustering	
2021	TPAMI	Single Model (in Feature Space)	Entropy	-	-				Hybrid - Fusion	
2021	TPAMI	-	-	-	Multivariate Radiomics Features Deep Saliency Features				Top-k	
2021	TPAMI	-	-	-	-				Top-k	✓

Table 2: Methodology summarization of surveyed active learning works.

Year	Venues	Uncertainty		Representativeness			Sampling Strategy	SemiSL	SelfSL	ADA	Region	Generative
		Method	Basic Metrics	Method	Basic Metrics	Basic Metrics						
2022	Kothawade et al. (2022b)	-	-	Cover-based - Submodular	Gradient	-	Top-k	-	-	-	-	-
2022	Xie et al. (2022b)	Single Model	Margin	Density-based	Energy	-	Hybrid - Multi-round	-	-	-	-	✓
2022	Wang et al. (2022b)	Gradient-based Metrics	Gradient	-	-	-	Top-k	-	-	-	-	-
2022	Liu et al. (2022a)	Multiple Inferences - Data Augmentations	Variance	-	-	-	Top-k	-	-	-	-	Pseudo-label
2022	Gong et al. (2022)	-	-	Discrepancy-based	MMD	-	Learnable - Reinforcement Learning & Meta Learning	-	-	-	-	-
2022	Xie et al. (2022d)	Single Model	Margin, Gradient	-	-	-	Top-k	-	-	-	-	✓
2022	Zhang et al. (2022a)	Single Model Adversarial Samples	Entropy KL Divergence	Density-based	Mean Cosine Similarity of KNN	-	Hybrid - Equal Split	-	-	-	-	Consistency
2022	Zhang et al. (2022b)	Single Model	Entropy	-	-	-	Top-k	-	-	-	-	✓
2022	Parvaneh et al. (2022)	Data Disagreement	Inequality	-	-	-	Diversity - Clustering	-	-	-	-	-
2022	Xie et al. (2022a)	Single Model	Entropy	-	-	-	Top-k	-	-	-	-	✓
2022	Qian et al. (2022)	-	-	Cover-based	Cosine Similarity	-	Top-k	-	-	-	-	Patch
2022	Wu et al. (2022a)	Single Model	Entropy	Discrepancy-based	Cosine Similarity	-	Class-balance	-	-	-	-	-
2022	Wang et al. (2022c)	-	-	Density-based	KNN Density	-	Diversity - Clustering w/ Regularization	-	-	-	-	✓
2022	Kothawade et al. (2022a)	-	-	Cover-based - Submodular	Cosine Similarity	-	Top-k	-	-	-	-	-
2022	Chen et al. (2022b)	Gradient-based Metrics	Gradient	-	-	-	Top-k	-	-	-	-	✓
2022	Hu et al. (2022)	Multiple Inferences - Data Augmentations	Entropy KL Divergence	-	-	-	Hybrid - Multi-round	-	-	-	-	Pseudo-label
2022	Hwang et al. (2022)	Single Model	Margin	Discrepancy-based	MMD	-	Hybrid - Multi-round	-	-	-	-	✓
2022	Yi et al. (2022)	Single Model	Least Confidence	Self-supervised Learning	Loss of Pretext Task	-	Hybrid - Multi-round	-	-	-	-	✓
2022	Wu et al. (2022b)	Single Model	Entropy	Density-based	GMM	-	Hybrid - Multi-round	-	-	-	-	✓
2022	Mahmood et al. (2022)	-	-	Discrepancy-based	Wasserstein Distance	-	Diversity - Solve Programming Problem	-	-	-	-	✓
2022	Hacohen et al. (2022)	-	-	Density-based	Inverse Average Distance to KNN samples	-	Diversity - Clustering	-	-	-	-	✓
2022	Jin et al. (2022a)	-	-	Clustering	Cosine Similarity	-	Diversity - Clustering	-	-	-	-	✓
2022	Jin et al. (2022c)	-	-	Clustering	L2 Distance	-	Class-balance	-	-	-	-	✓
2022	Jin et al. (2022b)	-	-	Clustering	L2 Distance	-	Diversity - Farthest-first Traversal	-	-	-	-	✓
2022	Dai et al. (2022)	Gradient-based Metrics	Gradient	-	-	-	Latent Space Optimization & Nearest Neighbour Search	-	-	-	-	Slice
2022	Zhou et al. (2022)	Performance Estimation - Learnable	Dice	-	-	-	Top-k	-	-	-	-	-
2022	Azzeni et al. (2022)	Performance Estimation - Surrogate	Dice	-	-	-	Top-k	-	-	-	-	-
2022	Nath et al. (2022)	Multiple Inferences - MC Dropout	Entropy	-	-	-	Top-k	-	-	-	-	Pseudo-label
2022	Balaram et al. (2022)	Uncertainty-aware Model - EDL	Entropy	-	-	-	Top-k	-	-	-	-	Pseudo-label & Consistency
2022	Wu et al. (2022c)	-	-	Cover-based	Cosine Similarity	-	Diversity - Clustering	-	-	-	-	Slice
2022	Bar et al. (2022)	Model Disagreement	Entropy-weighted Dice Distance	-	-	-	Hybrid - Fusion	-	-	-	-	Pseudo-label
2022	Kothawade et al. (2022c)	-	-	Cover-based - Submodular	Gradient	-	Top-k	-	-	-	-	-
2022	Yehuda et al. (2022)	-	-	Cover-based	L2 Distance	-	Graph-based Algorithm	-	-	-	-	-
2022	Mahapatra et al. (2022)	-	-	Saliency Maps	Graph-based Methods	-	Top-k	-	-	-	-	Pseudo-label
2022	Li et al. (2022)	Curriculum Learning & Noisy Sample Detection	Entropy	-	-	-	Top-k	-	-	-	-	-
2022	Bengar et al. (2022)	Single Model	Entropy	-	-	-	Class-balance	-	-	-	-	-
2023	Xie et al. (2023b)	-	-	Discrepancy-based	Wasserstein Distance	-	Latent Space Optimization & Nearest Neighbour Search	-	-	-	-	✓
2023	Lyu et al. (2023)	Data Disagreement	Cross Entropy, Variance	-	-	-	Hybrid - Fusion	-	-	-	-	Pseudo-label
												Box

Table 2: Methodology summarization of surveyed active learning works.

Year	Venues	Uncertainty		Representativeness			SemiSL	SelfSL	ADA	Region	Generative
		Method	Method	Basic Metrics	Method	Basic Metrics					
2023	CVPR	Single Model	Entropy	Discrepancy-based	H-Divergence	Diversity - Clustering	✓				
2023	CVPR	Single Model	IoU Confidence	-	-	Diversity - Clustering	✓				
2023	ICLR	Multiple Inferences - Model Ensemble	Entropy, Variance Ratio, BALD, Margin	-	-	Top-k					
2023	ICLR	Uncertainty-aware Model - EDL	Mutual Information & Entropy Expectation of Dirichlet Distribution	-	-	Hybrid - Multi-round	✓				
2023	ICCV	Single Model	BvSB	-	-	Class-balance					Superpixel
2023	ICLR	Uncertainty-aware Model - EDL	Mutual Information	-	-	Top-k					
2023	ICLR	Uncertainty-aware Model - EDL	Evidential Uncertainty	Density-based	Inverse Average Distance	Hybrid Fusion					
2023	ISBI	Multiple Inferences - MC Dropout Model Disagreement	Variance Inequality	-	-	Hybrid - Fusion					
2023	MIDL	-	-	Loss of Self-supervised Pretext Tasks	-	Diversity - Clustering	✓				
2023	TMI	-	-	Clustering	Consistency	Diversity - Clustering					✓
2023	TPAMI	-	-	Discrepancy-based	Semantic and distinctive scores	Hybrid - Fusion	✓				
2023	TPAMI	Adversarial Training	Disagreement of Classifiers	-	-	Top-k					

further selected less consistent samples for annotation. Results showed that combining AL with semi-supervised learning significantly improves performance.

Additionally, some works integrated existing consistency-based semi-supervised methods into the training process of AL. Huang et al. (2021) combined their proposed COD with MeanTeacher (Tarvainen and Valpola, 2017), demonstrating superior performance. Both TypiClust (Hacohen et al., 2022) and ProbCover (Yehuda et al. (2022) found that their methods outperformed other active learning baselines in low-budget scenarios when combined with FlexMatch (Zhang et al., 2021). Wang et al. (2022c) combined density-based AL with different existing semi-supervised methods. Results showed that the proposed method outperforms other active learning methods and excels in semi-supervised learning. Zhang et al. (2022a) combined AL with both pseudo-labeling and consistency. The unlabelled images first underwent both strong and weak data augmentations. When the confidence level of the weakly augmented images exceeded a certain threshold, they used these samples for semi-supervised training. Specifically, predictions of the weakly augmented images were assigned as pseudo-labels, and the outputs of the strongly augmented images were forced to be consistent with the pseudo-labels. However, when the confidence level was lower than the threshold, they used these samples for AL. A balanced uncertainty selector and an adversarial instability selector were used to select samples for oracle annotation. They validated the effectiveness of their proposed method in grading metastatic epidural spinal cord compression with MRI images.

4.2. Self-supervised Learning: Utilizing Pre-trained Model

In the last section, we discussed the integration of AL and semi-supervised learning, which aimed to utilize unlabeled data for better performance. However, the effectiveness of this approach is constrained by the size of dataset. This limitation is particularly evident in medical image analysis, where datasets are often relatively small. To further improve annotation efficiency, AL can be combined with self-supervised learning. Self-supervised learning (Liu et al., 2021a) trained the model with the supervision from the data itself, thus allowing pre-training on a large dataset. After finetuning on a few randomly selected labeled samples, the self-supervised pre-trained models have been shown to achieve impressive performance (Chen et al., 2020). Besides, these models can also provide good initialization, thereby solving the cold-start problem in AL. In this section, we will first introduce how self-supervised models solve the cold-start problem in AL and then explore different ways of integrating active learning with self-supervised learning.

4.2.1. Cold-start Problem in Active Learning

Current AL methods usually require several initial labeled samples to train an initial model and ensure reliable informativeness metrics. However, when the initial labeled set is small or even absent, the performance of these AL methods

drops dramatically, sometimes even worse than random sampling (Chen et al., 2023; Hacohen et al., 2022; Yehuda et al., 2022). This is known as the cold-start problem in AL, which is very common in AL. In their semi-supervised active learning framework, Gao et al. (2020) found that performance suffered with a smaller labeling budget compared to a larger one when initial labels were randomly selected. Bengar et al. (2021) first pre-trained the model with self-supervised learning and then employed some AL baselines to select samples for labeling and finetuning. Results showed the performance of AL baselines tends to be worse than the random selection under the low-budget scenario. Additionally, Xie et al. (2023a) discovered that CoreSet based on self-supervised features is inferior to random sampling. Tackling the cold-start problem is vital for improving the efficacy of AL, especially when the annotation budget is limited. Moreover, when constructing a new dataset from scratch, employing cold-start AL strategies can offer a good initialization, thereby boosting performance.

A key solution to the cold-start problem in AL lies in selecting the optimal set of initial labeled samples. Since no initial labels are available, cold-start AL requires different strategies than existing AL methods. Self-supervised pre-trained models offer a good initialization for effectively tackling the cold-start problem in AL. In natural language processing, Yuan et al. (2020) was the first to introduce the cold-start problem in AL. They employed self-supervised pre-trained models to address this issue. Yi et al. (2022) chose initial samples based on the loss of self-supervised pretext tasks, showing significant advantages over random sampling. Pourahmadi et al. (2021) proposed a straightforward baseline for cold-start active learning. They first performed k-Means clustering on existing off-the-shelf self-supervised features, then selected cluster centers for annotation. Results indicated that this baseline is very effective when the annotation budget is limited. TypiClust (Hacohen et al., 2022) found that when the annotation budget is low, querying typical samples is more beneficial, whereas when the budget is high, querying hard samples is more beneficial. This conclusion suggested different strategies with uncertainty methods for cold-start AL. Thus, based on self-supervised features, TypiClust selected samples from high-density areas of each k-Means cluster. Yehuda et al. (2022) employed a graph-based greedy algorithm to select the optimal initial samples based on self-supervised features. Chen et al. (2023) found that active learning also suffers from a cold-start problem in medical image analysis. The issues arose mainly because AL is often biased towards specific classes, resulting in class imbalance. Additionally, the models struggled to detect anomalies when only a limited number of initially labeled samples exist. They combined clustering and the loss of contrastive learning to address the cold-start problem. In CT segmentation, Nath et al. (2022) designed new pretext tasks for self-supervised pre-training. The model was trained to learn the threshold segmentation by an abdominal soft-tissue window. Results indicated that the proposed method significantly outperforms random sampling in selecting initial samples.

Additionally, some works have attempted to use fully

supervised pre-trained models to address the cold-start problem. Zhou et al. (2017) and their subsequent work (Zhou et al., 2021b) used ImageNet pre-trained models to select samples for labeling from completely unlabeled datasets. They combined entropy and disagreement as informativeness metrics, where the disagreement was the KL divergence of prediction probabilities between different patches of the same sample. They also introduced randomness to balance exploration and exploitation.

4.2.2. Combination of Active Learning and Self-supervised Learning

Features: The simplest way to integrate AL with self-supervised learning is by leveraging the high-quality pre-trained features that effectively capture data similarities. In point cloud segmentation, Hou et al. (2021) performed k-Means clustering on the self-supervised features, then selected the points of cluster centers for annotation. They improved the annotation efficiency in indoor scene point cloud segmentation.

Pretext tasks: In addition, the pretext tasks in self-supervised learning can be used for AL. They are tasks for which the supervision comes directly from the data itself. Different pretext tasks correspond to different pre-training paradigms. Typical pretext tasks include rotation prediction (Gidaris et al., 2018), colorization (Zhang et al., 2016), jigsaw puzzles (Noroozi and Favaro, 2016), contrastive learning (He et al., 2020), and masked modeling (He et al., 2022), etc. Solving these pretext tasks on extensive unlabeled data, the model acquires useful feature representations that can indirectly reflect data characteristics. Related works generally employed the loss of pretext task for AL. Yi et al. (2022) found a strong correlation between the loss of pretext tasks and the loss of downstream tasks. Thus, they initially focused on annotating samples with higher loss of pretext tasks and later shifted to those with lower loss. Results showed that rotation prediction performed the best among different pretext tasks. In Chen et al. (2023), the loss of contrastive learning was used for AL. They assumed that samples with higher losses are more representative of the data distribution. Specifically, they pre-trained on the target dataset using MoCo (He et al., 2020) for contrastive learning and then used k-Means clustering to partition the unlabeled data into multiple clusters, selecting the samples with the highest contrastive loss within each cluster for annotation. They then selected samples with the highest contrastive loss in each cluster for annotation.

Others: Furthermore, we can also leverage self-supervised learning in other ways for AL. In classification tasks, Zhang et al. (2022b) introduced one-bit annotation into AL for classification tasks. Firstly, they selected informative samples through uncertainty metrics. Oracles returned whether the current prediction was right or wrong rather than full annotation. Then, contrastive learning was adopted to pull the correct predictions closer to their corresponding classes and push away wrongly predicted samples from the predicted classes. Results indicated that the proposed method outperforms other AL methods regarding bit information. Du et al. (2021) integrated

contrastive learning into AL to tackle the problem of class distribution mismatch, where unlabeled data often includes samples out of the class distribution of the labeled dataset. In this work, contrastive learning filtered samples of mismatched classes that differ from the current class distribution. Besides, contrastive learning highlighted samples' informativeness by setting carefully designed negative samples. Their extended work Du et al. (2022) provided more theoretical analysis and experimental results and further integrated existing label information into the contrastive learning framework.

4.3. Active Domain Adaptation: Tackling Distribution Shift

Domain Adaptation (DA) (Guan and Liu, 2021) has wide applications in medical image analysis and computer vision. It aims to transfer knowledge from the source to the target domain, thus minimizing annotation costs. Currently, the most common setting of DA is unsupervised domain adaptation (UDA), in which the source domain is labeled while the target domain is unlabeled. However, the performance of UDA still lags behind fully supervised learning in the target domain (Liu et al., 2023). To bridge this gap, a natural idea would be to employ AL to select and annotate informative samples in the target domain. This setting is known as active domain adaptation (ADA). For better queries in ADA, one should consider uncertainty and whether the sample represents the target domain. The latter is commonly referred to as domainness or targetness in ADA. This section reviews the development of ADA and explores various ways of integrating AL with DA.

Su et al. (2020) was the first to introduce the concept of ADA and combined domain adversarial learning with AL. Through a domain discriminator and task model, they performed importance sampling to select target domain samples that are uncertain and highly different from the source domain. Fu et al. (2021) combined query-by-committee, uncertainty, and domainness for selecting the most informative samples under distribution shift. They adopted a domain discriminator to select samples with high domainness and employed Gaussian kernels to filter out anomalous and source-similar samples of the target domain. Random sampling was also used to improve diversity. Prabhu et al. (2021) performed k-Means clustering on target domain samples and selected cluster centers for annotation. The cluster centers were weighted by uncertainty, thus ensuring that selected samples were uncertain and diverse. Rangwani et al. (2021) formulated ADA as a submodular optimization problem. The sum of uncertainty, diversity, and representativeness was considered the gain for annotating a sample. Specifically, uncertainty was measured by the KL divergence between the original samples and their adversarial samples. Diversity was defined as the minimum KL divergence from a single sample to a set of samples. The Bhattacharya coefficient between samples was used as the representativeness score. They adopted a greedy algorithm to iteratively pick samples with the maximum gain. In segmentation tasks, Ning et al. (2021) introduced the idea of anchors in ADA. They concatenated features of different classes from the source domain images. Cluster centers of these concatenations were referred to as anchors. They then computed the distance

between each target sample and its nearest anchor. Target samples with the highest distance were requested for annotation. [Shin et al. \(2021\)](#) proposed LabOR, which first used a UDA pre-trained model to generate pseudo-labels for target samples and trained two segmentation heads with these pseudo-labels. They maximized the disagreements between the two heads and annotated regions that exhibited the most disagreement. LabOR achieved performance close to full supervision with only 2.2% of target domain annotations. [Hwang et al. \(2022\)](#) first selected representative samples in the target domain with maximum mean discrepancy. Uncertain ones within these samples were sent for annotation, while the confident ones are used for pseudo-labels. [Xie et al. \(2022b\)](#) introduced the concept of energy ([LeCun et al., 2006](#)) into ADA. The energy is inversely proportional to the likelihood of the data distribution. In this work, the model trained on the source domain was used to calculate the energy of target domain samples. Samples with high energy were selected for annotation, which suggested they are representative of the target domain and substantially different from the source data. [Xie et al. \(2022d\)](#) spotted the hard source samples by maximizing margin loss and leveraged these samples to select target samples close to the decision boundary. Based on EDL, [Xie et al. \(2022c\)](#) incorporated Dirichlet distribution to mitigate model miscalibration on the target domain. Distribution and data uncertainty were both used for sample selection. [Huang et al. \(2023\)](#) selected samples with high uncertainty and prediction inconsistency to their nearest prototypes. In 3D object detection, [Yuan et al. \(2023\)](#) adopted a diversity-based strategy to select target domain samples. Specifically, they first clustered samples based on similarity and selected prototypes of each cluster for annotation.

4.4. Region-based Active Learning: Smaller Labeling Unit

Most AL works require the oracle to label the full image in medical image analysis and computer vision. However, labeling a full image can introduce redundancy in fine-grained tasks like segmentation and detection, resulting in an inefficient use of the annotation budget. For example, in segmentation tasks of autonomous driving, large areas in the image (e.g., roads) do not need exhaustive annotation. Instead, those annotation budgets would be better spent on detailed smaller areas, such as pedestrians or utility poles. An image can be divided into non-overlap regions to further improve annotation efficiency, and experts can opt to annotate specific regions within an image. This method is termed as “region-based active learning”. This section introduces region-based active learning from three perspectives: patches, superpixels, and region-based active domain adaptation.

4.4.1. Patches

Patches are most commonly used in region-based active learning, generally represented as square boxes. [Mackowiak et al. \(2018\)](#) combined uncertainty and annotation cost to select the informative patches for annotation. [Casanova et al. \(2020\)](#) employed deep reinforcement learning to automatically select informative patches for annotation. In retinal blood

vessels segmentation of eye images, [Xu et al. \(2021\)](#) selected patches with the highest uncertainty for annotation. Furthermore, they utilized latent-space Mixup to encourage linearization between labeled and unlabeled samples, thus leveraging unlabeled data to improve performance.

4.4.2. Superpixels

Superpixels are also widely used in region-based active learning. Superpixel generation algorithms ([Achanta et al., 2012](#); [Van den Bergh et al., 2012](#)) over-segment images based on color and texture, grouping similar pixels into the same superpixel. Superpixel-based AL initially pre-segments the images and then calculates the informativeness of each superpixel. The informativeness metric of each superpixel is the average of its constituent pixels. [Kasarla et al. \(2019\)](#) introduced a baseline method for selecting superpixels based on uncertainty. In multi-view indoor scene segmentation, [Siddiqui et al. \(2020\)](#) adopted uncertainty and disagreement between different viewpoints to select informative superpixels for annotation. [Cai et al. \(2021\)](#) utilized uncertainty as the informativeness metric. They introduced a class-balanced sampling strategy to better select superpixels containing minority classes. Furthermore, they adopted a “dominant labeling” scheme. The dominant labeling is the majority class label of all pixels in the superpixel. They assigned the dominant labeling to every pixel within a superpixel, thus eliminating the need for detailed delineation. Results showed that, with the same number of labeling clicks, dominant labeling at the superpixel level significantly outperforms precise labeling at the patch level. As a follow-up, [Kim et al. \(2023\)](#) proposed to adaptively merge and split spatially adjacent, similar, and complex superpixels, respectively. This approach yielded better performance than ([Cai et al., 2021](#)) with dominant labeling. In 3D vision, similar over-segmentation has also been applied to point clouds segmentation by [Wu et al. \(2021a\)](#), [Hu et al. \(2022\)](#) and [Liu et al. \(2022a\)](#). The former two works adopted supervoxel segmentation algorithms, while the latter employed k-Means for over-segmentation.

4.4.3. Region-based Active Domain Adaptation

To better utilize the annotation budget, some ADA segmentation works also employed patches or superpixels for annotation. In [Xie et al. \(2022a\)](#), uncertainty and regional impurity were used to select and annotate the most informative patches. Regional impurity measured the number of unique predicted classes within the neighborhood of a pixel, which presents the edge information. They used extremely small patches (e.g., size of 3x3) for annotation and achieved performance close to full supervision with only 5% of the annotation cost. [Wu et al. \(2022b\)](#) proposed a density-based method to select the most representative superpixels in the target domain for annotation. They employed Gaussian mixture models (GMM) as density estimators for superpixels in both the source and target domains, aiming to select those with high density in the target domain and low density in the source domain.

4.5. Generative Model: Data Augmentation and Generative Active Learning

In recent years, the advancement of deep generative models enabled high-quality generation and flexible conditional generation. For example, a trained model could generate the corresponding lung X-ray scan when conditioned on a lung mask. By integrating generative models, we can further improve the annotation efficiency of AL. In this section, we discuss how AL can be combined with generative models from two aspects: data augmentation and generative active learning.

4.5.1. Synthetic Samples as Data Augmentation

The simplest approach considers the synthetic sample produced by generative models as advanced data augmentation. These methods utilize label-conditioned generative models. As a result, it's guaranteed that all synthetic samples are correctly labeled since specifying the labels is a prerequisite for data generation. This method enables us to acquire more labeled samples without any additional annotations. [Tran et al. \(2019\)](#) argued that most synthetic samples produced by generative models are not highly informative. Therefore, they first adopted the BALD uncertainty to select samples for annotation, then trained a VAE-ACGAN on these labeled data to generate more informative synthetic samples. [Mahapatra et al. \(2018\)](#) used conditional GANs to generate chest X-rays with varying diseases to augment the labeled dataset. Then, MC Dropout was used to select and annotate highly uncertain samples. With the help of AL and synthetic samples, they achieved performance near fully supervised using only 35% of the data. Training conditional generative models require a large amount of labeled data, while the labeled dataset in AL is often relatively small. To address this issue, [Lou et al. \(2023\)](#) proposed a conditional SinGAN ([Shaham et al., 2019](#)) that only requires one pair of images and masks for training. The SinGAN improved the annotation efficiency for nuclei segmentation. Additionally, [Chen et al. \(2022b\)](#) integrated implicit semantic data augmentation (ISDA) ([Wang et al., 2021](#)) into AL. They initially used ISDA to augment unlabeled samples, then selected samples with large diversity between different data augmentations for annotation. The model is trained on both the original data and its augmentations.

4.5.2. Generative Active Learning

Generative active learning selects synthetic samples produced by generative models for oracle annotation, thus without requiring a large unlabeled sample pool. The advantage of this approach lies in its ability to continuously search the data manifold through generative models. It's worth noting that works in this section follow the setting of membership query synthesis, while works in the last section follow the setting of pool-based active learning. This distinction arises because generative models in the last section were solely utilized to augment existing labeled datasets. [Zhu and Bento \(2017\)](#) attempted to generate uncertain samples with GAN for expert annotation. Unfortunately, the quality of the generated samples was low and included many samples

with indistinguishable classes. Since experts find it difficult to annotate low-quality synthetic samples, alternative methods are needed to annotate these samples. [Chen et al. \(2021\)](#) first trained a bidirectional GAN to learn the data manifold. They then selected uncertain areas in the feature space and generated images within these regions using bidirectional GAN. Finally, they used physics-based simulation to provide labels for the generated samples. In calcification level prediction in aortic stenosis of CT, they improved annotation efficiency by up to 10 times compared to random generation.

5. Active Learning for Medical Image Analysis

Due to the potential of significantly reducing annotation costs, AL is receiving increasing attention in medical image analysis. The unique traits of medical imaging require us to design specialized AL methods. Building on the foundation of the previous two sections, this section will focus on introducing AL works tailored to medical image analysis across different tasks, including classification, segmentation, and reconstruction. Additionally, in [Table 3](#), we list all the AL works related to medical image analysis in this survey, providing the name of the used dataset, its modality, ROIs, and corresponding clinical and technical tasks.

5.1. Active Learning in Medical Image Classification

Some common clinical tasks, such as disease diagnosis, cancer staging, and prognostic prediction, can be formulated as medical image classification. Most AL works in medical imaging classification directly employ general methods, such as using class-balancing sampling in [§3.3.2](#) to mitigate the long-tail effect of medical imaging datasets. However, specialized design of AL algorithms is required for certain modalities of medical image classification. For example, the classification of chest X-rays often involves the idea of multi-label. Besides, classifying pathological whole-slide images typically needs to be formulated as a multiple instance learning problem. This section will introduce AL works specifically targeted at classification problems in chest X-rays and pathological whole-slide images.

5.1.1. Chest X-ray and Multi-label Classification

Chest X-ray examinations are crucial for screening and diagnosing lung, cardiovascular, skeletal, and other thoracic diseases. Computer-aided diagnosis in this domain has been extensively researched, including AL works aimed at reducing annotation costs for physicians. [Mahapatra et al. \(2021\)](#) introduced saliency maps to select informative samples for annotation. To aggregate the per-pixel saliency maps into a single scalar, they explored three different approaches, including computing the kurtosis of the saliency map, utilizing multivariate radiomic features, and combining deep features of autoencoders and clustering. Results demonstrated that the aggregation using deep features performs the best. [Nguyen et al. \(2021\)](#) introduced a gist-set to select samples near the decision boundary. Besides, uncertain samples with high entropy were

Table 3: Surveyed Works of Active Learning related to Medical Image Analysis.

Year	Venues	Modality	ROIs	Dataset	Clinical Task	Technical Task
Zhou et al. (2017)	2017 CVPR	Colonoscopy Colonoscopy CT	Colon Colon Lung	in-house in-house in-house	Image Quality Assessment Polyp Detection Pulmonary Embolism Detection	Classification Classification Classification
Gal et al. (2017)	2017 ICML	Dermoscopy	Skin	ISIC 2016	Skin Cancer Diagnosis	Classification
Yang et al. (2017)	2017 MICCAI	Histopathology Ultrasound	Colon Lymph Node	Glas in-house	Gland Segmentation Lymph Node Segmentation	Segmentation Segmentation
Beluch et al. (2018)	2018 CVPR	Fundus	Eye	EyePacs	Diabetic Retinopathy Detection	Classification
Xu et al. (2018)	2018 CVPR	Histopathology	Colon	Glas	Gland Segmentation	Segmentation
Sourati et al. (2018) Sourati et al. (2019)	2018 DLMIA 2019 TMI	MRI	Brain	dHCP & in-house	Brain Extraction	Segmentation
Kuo et al. (2018)	2018 MICCAI	CT	Head	in-house	Intracranial Hemorrhage Detection	Segmentation
Mahapatra et al. (2018)	2018 MICCAI	X-ray	Chest	SCR & Chestx-ray8	Lung Segmentation Thoracic Disease Diagnosis	Segmentation Classification
Jin et al. (2019)	2019 arXiv	MRI	Heart Knee	Cardiac Atlas Project fastMRI	MRI Reconstruction MRI Reconstruction	Reconstruction Reconstruction
Zheng et al. (2019)	2019 AAAI	Histopathology MRI Electron Microscopy	Colon Heart Fungus	Glas HVSMMR 2016 in-house	Gland Segmentation Whole-heart Segmentation Fungus Segmentation	Segmentation Segmentation Segmentation
Zhang et al. (2019)	2019 CVPR	MRI	Knee	fastMRI	MRI Reconstruction	Reconstruction
Qi et al. (2019)	2019 JBHI	Histopathology	Breast	BreaKHis	Breast Cancer Diagnosis	Classification
Sadafi et al. (2019)	2019 MICCAI	Microscopy	Blood	in-house	Red Blood Cell Detection	Object Detection
Zheng et al. (2020)	2020 AAAI	MRI Electron Microscopy	Heart Mouse	HVSMMR 2016 Lee et al. (2015)	Whole-heart Segmentation Neuron Boundary Segmentation	Segmentation Segmentation
Lin et al. (2020)	2020 ECCV	Electron Microscopy	Mouse Synapses & Mitochondria	EM-R50	Synapse Detection & Mitochondria Segmentation	Segmentation
Dai et al. (2020)	2020 MICCAI	MRI	Brain	BraTS 2019	Brain Tumor Segmentation	Segmentation
Li and Yin (2020)	2020 MICCAI	Histopathology MRI	Colon Brain	Glas iSeg	Gland Segmentation Infant Brain Segmentation	Segmentation Segmentation
Liu et al. (2020)	2020 MICCA	CT	Lung	DeepLesion	Pulmonary Nodule Detection	Object Detection
Mi et al. (2020)	2020 MICCAI	Electron Microscopy	Mouse Cortex Human Cerebrum	SNEMI3D in-house	Accelerated Acquisition of Electron Microscopy	Reconstruction Reconstruction
Pineda et al. (2020)	2020 MICCAI	MRI	Knee	fastMRI	MRI Reconstruction	Reconstruction
Shen et al. (2020)	2020 MICCAI	Immunohistochemistry	Breast	in-house	Breast Cancer Region Segmentation	Segmentation
Wang et al. (2020a)	2020 MICCAI	CT Fundus	Lung Eye	Tianchi EyePacs	Lung Disease Detection Diabetic Retinopathy Detection	Classification Classification
Bakker et al. (2020)	2020 NeurIPS	MRI	Knee Brain	fastMRI fastMRI	MRI Reconstruction MRI Reconstruction	Reconstruction Reconstruction
Hiasa et al. (2020)	2020 TMI	CT	Hip & Thigh	TCIA & in-house	Muscle Segmentation	Segmentation

Table 3: Methodology summarization of surveyed active learning works.

Year	Venues	Modality	ROIs	Dataset	Clinical Task	Technical Task
Huang et al. (2020)	TMI	X-ray	Chest	in-house	Rib Fracture Recognition	Object Detection
Zhao et al. (2021)	JBHI	Dermoscopy X-ray	Skin Hand	ISIC 2017 RSNA Bone Age Dataset	Skin Lesion Segmentation Finger Bone Segmentation	Segmentation Segmentation
Wu et al. (2021b)	MedIA	CT	Lung	CC-CCLII	COVID-19 Diagnosis	Classification
Zhou et al. (2021b)	MedIA	Colonoscopy Colonoscopy CT	Colon Colon Lung	in-house in-house in-house	Image Quality Assessment Polyp Detection Pulmonary Embolism Detection	Classification Classification Classification
Wang and Yin (2021)	MICCAI	Microscopy (Synthetic) Histopathology Histopathology	Bacterial Cells Human Bone Marrow Human Adipocyte Cells Various Tissues & Species	VGG Cell MBM ADI DCC	Cell Counting Cell Counting Cell Counting Cell Counting	Keypoint Localization Keypoint Localization Keypoint Localization Keypoint Localization
Xu et al. (2021)	MICCAI	Fundus OCTA	Eye Eye	DRIVE ROSE-1	Retina Vessel Segmentation Retina Vessel Segmentation	Segmentation Segmentation
Zhou et al. (2021a)	MICCAI	CT	Lung Colon Kidney	MSD MSD KiTS 19	Tumor Segmentation Tumor Segmentation Kidney & Tumor Segmentation	Segmentation Segmentation Segmentation
Nguyen et al. (2021)	MIDL	X-ray	Chest Chest Chest	in-house RSNA Pneumonia CheXpert	Diagnosis of Airspace Opacity & Lung Lesion Diagnosis of Pneumonia Detection of Pleural Effusion	Classification Classification Classification
Mahapatra et al. (2021)	TMI	X-ray Histopathology	Chest Colon	ChestX-ray8 Glas	Thoracic Disease Diagnosis Gland Segmentation	Classification Segmentation
Nath et al. (2021)	TMI	CT MRI	Pancreas Hippocampus	MSD MSD	Pancreas & Tumor Segmentation Hippocampus Segmentation	Segmentation Segmentation
Chen et al. (2021)	TPAMI	CT	Heart	in-house	Calcification Level Prediction in Aortic Stenosis	Classification
Wang et al. (2022a)	arXiv	CT	Lung Spine	AAPM VerSe	CT Reconstruction CT Reconstruction	Reconstruction Reconstruction
Kothawade et al. (2022b)	AAAI	X-ray	Chest	PneumoniaMNIST	Pneumonia & Normal Classification	Classification
Quan et al. (2022)	CVPR	X-ray	Head Hand	Kaggle Payer et al. (2019)	Cephalometric Landmark Detection Hand Landmark Detection	Keypoint Localization Keypoint Localization
Zhang et al. (2022a)	CVPR	MRI	Spine	in-house	Diagnosis of Metastatic Epidural Spinal Cord Compression	Classification
Jim et al. (2022c)	Knowledge-based Systems	Dermoscopy	Skin	ISIC 2020	Skin Lesion Classification	Classification
Jim et al. (2022b)	Knowledge-based Systems	Dermoscopy X-ray	Skin Chest	ISIC 2018 Jaeger et al. (2013)	Skin Lesion Segmentation Lung Segmentation	Segmentation Segmentation
Atzeni et al. (2022)	MedIA	MRI Histology	Brain Brain	SATA in-house	Brain Structure Segmentation Brain Structure Segmentation	Segmentation Segmentation
Dai et al. (2022)	MedIA	MRI	Brain Brain	BraTS 2019 MALLC	Brain Tumor Segmentation Brain Structure Segmentation	Segmentation Segmentation
Zhou et al. (2022)	MedIA	CT CT CT Colonoscopy	Lung Colon Kidney Colon	MSD MSD KiTS 19 CVC-ClinicDB	Tumor Segmentation Tumor Segmentation Kidney & Tumor Segmentation Polyp Segmentation	Segmentation Segmentation Segmentation Segmentation

Table 3: Methodology summarization of surveyed active learning works.

Year	Venues	Modality	ROIs	Dataset	Clinical Task	Technical Task
Nath et al. (2022)	MICCAI	CT	Liver Hepatic Vessels	MSD MSD	Liver & Tumor Segmentation Hepatic Vessels & Tumor Segmentation	Segmentation Segmentation
Bai et al. (2022)	MICCAI	Wireless Capsule Endoscopy	Colon	CAD-CAP	Polyp Segmentation	Segmentation
Balaram et al. (2022)	MICCAI	X-ray	Chest	Chestx-ray8	Thoracic Disease Diagnosis	Classification
Wu et al. (2022c)	MICCAI	CT, MRI CT CT	Liver Liver Liver Liver	LiTS CHAOS Sliver07 MSD	Liver & Tumor Segmentation Liver & Tumor Segmentation Liver & Tumor Segmentation Liver & Tumor Segmentation	Segmentation Segmentation Segmentation Segmentation
Kothawade et al. (2022c)	MICCAIW	X-ray Histopathology Mircoscopy Dermoscopy Fundus	Chest Colon Peripheral Blood Skin Eye	PneumoniaMNIST PathMNIST BloodMNIST ISIC 2018 APTOS-2019	Pneumonia & Normal Classification Survival Prediction Cell Type Classification Skin Lesion Diagnosis Diabetic Retinopathy Detection	Classification Classification Classification Classification Classification
Li et al. (2022)	TMI	Histopathology	Prostate	PANDA	Gleason Grading of Prostate Cancer	Classification
Mahapatra et al. (2022)	TMI	X-ray	Chest	ChestXpert	Thoracic Disease Diagnosis	Classification
Jin et al. (2023b)	EAAI	Dermoscopy X-ray	Skin Chest	ISIC 2018 Jaeger et al. (2013)	Skin Lesion Segmentation Lung Segmentation	Segmentation Segmentation
Sadafi et al. (2023)	ISBI	Histopathology	Breast	CAMELYON17	Detection of Cancer Metastasesin Lymph Nodes	Classification
Qu et al. (2023)	MICCAI	Histopathology	Colon	NCT-CRC-HE-100K	Colorectal Cancer Diagnosis	Classification
Chen et al. (2023)	MIDL	Histopathology CT Mircoscopy	Colon Abdomen Peripheral Blood	PathMNIST OrganAMNIST BloodMNIST	Survival Prediction Classification of Body Organs Cell Type Classification	Classification Classification Classification
Lou et al. (2023)	TMI	Histopathology	Seven Organs Breast Seven Organs	TCGA-KUMAR TNBC MoNuSeg	Nuclei Segmentation Nuclei Segmentation Nuclei Segmentation	Segmentation Segmentation Segmentation

sent for annotation, while the confident samples were assigned as pseudo-labels. Additionally, they adopted momentum updates to enhance the stability of the sample predictions.

However, multiple diseases and abnormalities often coexist simultaneously in diagnosing chest X-rays. Therefore, multi-label classification has been introduced, allowing each sample to be categorized into multiple classes (Baltruschat et al., 2019). Consequently, AL algorithms for chest X-ray classification must adapt to the multi-label setting. Balaram et al. (2022) modified the EDL-based AL to accommodate the multi-label setting. Specifically, they transformed the Dirichlet distribution in EDL into multiple Beta distributions, each corresponding to one class label. They then calculated the entropy of the Beta distributions as the aleatoric uncertainty of the sample. Additionally, they incorporated semi-supervised methods like MeanTeacher (Tarvainen and Valpola, 2017), VAT (Miyato et al., 2018), and NoTeacher (Unnikrishnan et al., 2021) to further reduce annotation costs. Built upon saliency maps, Mahapatra et al. (2022) further introduced GNN to model the inter-relationships between different labels. In this work, each class was treated as a node in a graph, with the relationships between classes represented as edges. They employed various techniques to aggregate information between different classes.

5.1.2. Pathological Whole-slide Images and Multiple Instance Learning

Compared to modalities like X-ray, CT, and MRI, pathological whole-slide images (WSIs) provide microscopic details at the cellular level, making them critically important for tasks such as cancer staging and prognostic prediction. However, WSIs are very large, with maximum resolutions reaching $100,000 \times 100,000$ pixels. To handle these large images for deep learning, WSIs are usually divided into many small patches. Fully supervised methods require annotations for each patch, resulting in high annotation costs. AL can effectively improve annotation efficiency. For instance, in classifying breast pathological images, Qi et al. (2019) used entropy as the uncertainty metric. Uncertain patches were sent for annotation, whereas those with low entropy were given pseudo-labels to assist training.

Nevertheless, pathologists might only provide WSI-level annotations in real-world clinical scenarios. Consequently, a prevailing direction in research is to formulate WSI classification as the weakly-supervised multi-instance learning (MIL) (Qu et al., 2022). In this framework, the entire WSI is viewed as a bag, and patches within each WSI are treated as instances within that bag. A well-trained MIL learner can automatically identify relevant patches based on WSI-level labels, thus significantly reducing annotation costs. For example, a trained MIL classifier can automatically spot related patches by annotating whether or not cancer metastasis is present in a WSI. Nonetheless, task-relevant patches are often outnumbered by irrelevant ones, making MIL convergence more challenging. In MIL-based pathological WSI classification, AL filters out irrelevant patches and selects informative patches for annotation. Qu et al. (2023) found that

in addition to patches related to the target (e.g., tumors, lymph nodes, and normal cells), WSIs contain many irrelevant patches (e.g., fat, stroma, and debris). Therefore, they adopted the open-set AL (Ning et al., 2022), in which the unlabeled pool contained both target and non-target class samples. They combined feature distributions with prediction uncertainty to select informative and relevant patches of the target class for annotation. Based on attention-based MIL, Sadafi et al. (2023) adopted MC Dropout to estimate both attention and classification uncertainties of each patch, then sent the most uncertain patches in each WSI for expert annotation.

5.2. Active Learning in Medical Image Segmentation

Segmentation is one of the most common tasks in medical image analysis, capable of precisely locating anatomical structures or pathological lesions. However, training a segmentation model requires pixel-level annotation, which is time-consuming and labor-intensive for doctors. Therefore, active learning has been widely used in medical image segmentation and has become an important method to reduce annotation costs. Based on the unique traits of medical imaging, this section will focus on specialized designs in AL for medical image segmentation, including slice-based annotation, one-shot annotation, and annotation cost.

5.2.1. Slice-based Annotation

In 3D modalities like CT and MRI, adjacent 2D slices often exhibit significant semantic redundancy. Consequently, annotating only the key slices of each sample can reduce annotation costs. Representativeness-based methods have been widely applied in this line of work. For instance, Zheng et al. (2020) utilized autoencoders to learn the semantic features of each slice, then selected and annotated key slices from axial, sagittal, and coronal planes with a strategy similar to RA. Specifically, they initially trained three 2D segmentation networks and one 3D segmentation network, where the inputs for the 2D networks are slices from different planes. These segmentation networks were used to generate four sets of pseudo-labels and subsequently to train the final 3D segmentation network. Results showed that this slice-based strategy outperforms uniform sampling. Building upon this method, Wu et al. (2022c) incorporated a self-attention module into the autoencoder to enhance slice-level feature learning. In recent years, uncertainty methods have been introduced for selecting key slices. In interactive segmentation of 3D medical images, Zhou et al. (2021a) and their subsequent work (Zhou et al., 2022) introduced a quality assessment module to provide a predicted average IoU score for each slice. They chose the slice with the lowest IoU score in each volume for the next round of interactive segmentation. In muscle segmentation of CT images, Hiasa et al. (2020) selected key slices and key regions. This work adopted clustering to select key slices and further selected regions with high uncertainty within each key slice for annotation.

5.2.2. One-shot Annotation

Currently, most AL works require multiple rounds of annotation. However, this setting may not be practical in medical image segmentation. Multi-round annotation requires physicians to be readily available for each round of labeling, which is unrealistic in practice. If physicians cannot complete the annotations on time, the AL process must be suspended. In contrast, one-shot annotation eliminates the need for multiple interactions with physicians. It also allows for selecting valuable samples in a single round, thus reducing time costs. Both one-shot annotation and cold-start AL aim to select the most optimal initial annotations. However, the former allows for a higher annotation budget and strictly limits the number of interactions with experts to just one. Most relevant works combine self-supervised features and specific sampling strategies to achieve one-shot annotation. For example, RA (Zheng et al., 2019) is one of the earliest works in one-shot AL for medical image segmentation. They applied the VAE feature and a representativeness strategy to select informative samples for annotation in one shot. RA performed excellently in segmenting gland of pathological images, whole-heart of MRI images, and fungal of electron microscopic images. Jin et al. (2022b) combined features of contrastive learning with farthest-first sampling to achieve one-shot annotation. The proposed method demonstrated effectiveness on the ISIC 2018 and lung segmentation datasets. Additionally, Jin et al. (2023b) utilized auto-encoding transformations for self-supervised feature learning. They selected and annotated samples with high density based on reachable distance.

5.2.3. Annotation Cost

Current AL works often assume equal annotation costs for each sample. Yet, this is not the case in medical image segmentation, where the time to annotate different samples can differ greatly. AL techniques can better support physicians by considering annotation costs (e.g., annotation time). Nevertheless, there is still limited research in this specific domain. In detecting intracranial hemorrhage of CT scans, Kuo et al. (2018) combined predictive disagreement with annotation time to select samples for annotation. Specifically, they adopted the Jensen-Shannon divergence to measure the disagreement between the outputs of multiple models. Annotation time for each sample was estimated by the length of the segmentation boundary and the number of connected components. In this work, AL was framed as a 0-1 knapsack problem, and dynamic programming is used to solve this problem for selecting informative samples. In brain structure segmentation, Atzeni et al. (2022) further considered the spatial relationships between multiple regions of interest to more accurately estimate the annotation cost. Moreover, the average Dice coefficient of previous rounds was used to predict the average Dice for current segmentation results. They selected and annotated regions that can maximize the average Dice.

5.3. Active Learning in Medical Image Reconstruction

AL can also be applied in medical image reconstruction. AL methods can help minimize the observations needed for

modalities that require a long imaging time. This accelerates the imaging process and shortens the waiting period for patients. In this section, we'll explore the application of AL in the reconstruction of MRI, CT, and electron microscopy.

Deep learning has been applied to accelerate MRI acquisition and reconstruction. A common practice is to reduce k-space sampling through a fixed mask and use a deep model to reconstruct the undersampled MRI (Qin et al., 2018). To further improve the imaging speed, learnable sampling in AL can be applied to select the next measurement locations in k-space. For example, Zhang et al. (2019) adopted adversarial learning to train an evaluator for selecting the next row in k-space. Pineda et al. (2020) utilized reinforcement learning to train a dual deep Q-network for active sampling in k-space. Bakker et al. (2020) adopted policy gradient in reinforcement learning to train a policy network for adaptive sampling in k-space. The reward for the policy network was based on the improvement in structural similarity before and after the acquisition. Additionally, Bakker et al. (2022) explored how to jointly optimize the reconstruction and acquisition networks.

In addition to MRI imaging, AL has been employed in CT reconstruction as illustrated by Wang et al. (2022a). They adaptively chose the scanning angles tailored to individual patients, leading to a reduction in both radiation exposure and scanning duration. In electron microscopy, Mi et al. (2020) initially enhanced low-resolution images to high-resolution and then predicted the location of region-of-interest and reconstruction error. A weighted DPP based on reconstruction error was applied to select pixels that needed rescanned. Results showed that weighted DPP maintained both low reconstruction error and spatial diversity.

6. Challenges and Future Perspectives

Currently, annotation scarcity is a significant bottleneck hindering the development of medical image analysis. AL improves annotation efficiency by selectively querying the most informative samples for annotation. This survey reviews the recent developments in deep active learning, focusing on the evaluation of informativeness, sampling strategies, integration with other label-efficient techniques, and the application of AL in medical image analysis. In this section, we will discuss the existing challenges faced by AL in medical image analysis and its future perspectives.

6.1. Towards Active Learning with Better Uncertainty

In AL, uncertainty plays a pivotal role. However, it would be beneficial if the uncertainty more directly highlighted the model's mistakes. We can enhance the model's performance by querying samples with inaccurate predictions.

Recently, many works have adopted learnable performance estimation for quality control of deep model outputs. For instance, the recently proposed segment anything model (SAM) (Kirillov et al., 2023) provides IoU estimates for each mask to evaluate its quality. In medical image analysis, automated quality control is critical to ensure the reliability

and safety of the deep model outputs (Kohlberger et al., 2012). For example, Wang et al. (2020c) employed deep generative models for learnable quality control in cardiac MRI segmentation, where the predicted Dice scores showed a strong linear relationship with the real ones. Additionally, Billot et al. (2023) used an additional neural network to predict the Dice coefficient of brain tissue segmentation results. Overall, learnable performance estimation can accurately predict the quality of model outputs. Hence, delving deeper into their potential for uncertainty-based AL is crucial to effectively tackle the issue of over-confidence.

Moreover, improving the probability calibration of model prediction is a promising way to mitigate the over-confidence issue. Calibration (Guo et al., 2017; Mehrtash et al., 2020) reflects the consistency between model prediction probabilities and the ground truth. A well-calibrated model should display a strong correlation between confidence and accuracy. For instance, if a perfect-calibrated polyp classifier gives an average confidence score of 0.9 on a dataset, it means that 90% of those samples should indeed have polyps. In reality, deep models generally suffer from the issue of over-confidence, which essentially means that they are not well-calibrated. Currently, only a few uncertainty-based AL works have considered probability calibration. For instance, Beluch et al. (2018) found that the model ensemble has better calibration than MC Dropout. Xie et al. (2022c) mitigated miscalibration by considering all possible prediction outcomes in the Dirichlet distribution. However, these methods are limited to proposing a better uncertainty metric and validating the calibration quality post-hoc. Existing calibration methods (Guo et al., 2017; Ding et al., 2021) directly adjusted the distribution of prediction probabilities. However, these methods require an additional labeled dataset, thus limiting their practical applicability. Therefore, integrating probability calibration into uncertainty-based AL represents a valuable research direction worth exploring.

6.2. Towards Active Learning with Better Representativeness

Representativeness-based AL effectively utilizes feature representations and data distributions for sample selection. Cover-based and diversity-based AL methods implicitly capture the data distribution, whereas density-based AL explicitly estimates it. However, the latter requires supplementary strategies to ensure diversity. As the core of density-based AL, density estimation in high-dimensional spaces has always been challenging. Popular density estimation methods, such as kernel density estimation and GMM, may face challenges in high-dimensional spaces. In future research, we can consider introducing density estimators tailored to high-dimensional spaces.

6.3. Towards Active Learning with Weak Annotation

In §4.4, we discuss region-based active learning, which only requires region-level annotation of a sample. However, annotating all pixels within the region is still needed. Some AL works have incorporated weak annotations to simplify the task for annotators. In object detection tasks, Vo et al. (2022)

trained deep models with image-level annotation. They selected samples with box-in-box prediction results and annotated them with bounding boxes. Moreover, Lyu et al. (2023) adopted disagreement to choose which objects are worth annotating. Rather than annotating all objects within the image, they only required box-level annotations for a subset of objects. In AL of instance segmentation, Tang et al. (2022) only required annotations for each object’s class label and bounding box, without the annotation of fine-grained segmentation masks. In future research, AL based on weak annotations is a direction worthy of in-depth exploration.

6.4. Towards Active Learning with Better Generative Models

In §4.5, we summarize the applications of generative models in AL. However, existing works have mainly focused on using GANs as sample generators. Recently, diffusion models (Kazerouni et al., 2023) have advanced in achieving state-of-the-art generative quality. Furthermore, text-to-image diffusion models, represented by Stable Diffusion (Rombach et al., 2022), have revolutionized the image generation domain. Their high-quality, text-guided generation results enable a more flexible image generation. Exploring the potential of diffusion models in deep AL is a promising avenue for future research.

6.5. Towards Active Learning with Foundation Models

With the rise of visual foundational models, such as contrastive language-image pretraining (CLIP) (Radford et al., 2021) and SAM (Kirillov et al., 2023), and large language models (LLMs) like GPT (OpenAI, 2023), deep learning in medical image analysis and computer vision is undergoing a paradigm shift. These foundational models (Bommasani et al., 2021) offer new opportunities for the development of AL.

AL is closely related to the training paradigms in deep learning of computer vision and medical image analysis. From the initial approach of train-from-scratch to the “pretrain-finetune” strategy using supervised or self-supervised pre-trained models, these paradigms usually require fine-tuning the entire network. Foundation models contain a wealth of knowledge. When combined with recently emerging parameter-efficient fine tuning (PEFT) or prompt tuning techniques (Hu et al., 2021; Jia et al., 2022), we can tune only a minimal subset of model weights (for example, 5%) for rapid transfer to downstream tasks. As the number of fine-tuned parameters decreases, AL has the potential to further reduce the number of required annotated samples. Therefore, it is essential to investigate the applicability of existing AL under PEFT or prompt tuning and explore the most suitable AL strategies for PEFT.

In natural language processing, LLMs have already taken a dominant role. Since most researchers cannot tune the LLMs, they rely on in-context learning, which provides LLMs with limited examples to transfer to downstream tasks. We believe that visual in-context learning will play a vital role in future research. Therefore, selecting the most suitable prompts for visual in-context learning will become an important research direction of AL.

7. Conclusion

Active learning is important to deep learning in medical image analysis since it effectively reduces the annotation costs incurred by human experts. This survey comprehensively reviews the core methods in deep active learning, its integration with different label-efficient techniques, and active learning works tailored to medical image analysis. We further discuss its current challenges and future perspectives. In summary, we believe that deep active learning and its application in medical image analysis hold important academic value and clinical potential, with ample room for further development.

Acknowledgments

This study was supported by the National Natural Science Foundation of China (Grant 82372097 and 82072021) and the Science and Technology Innovation Plan of Shanghai Science and Technology Commission (Grant 23S41900400).

References

- Achanta, R., Shaji, A., Smith, K., Lucchi, A., Fua, P., Süsstrunk, S., 2012. Slic superpixels compared to state-of-the-art superpixel methods. *IEEE transactions on pattern analysis and machine intelligence* 34, 2274–2282.
- Agarwal, S., Arora, H., Anand, S., Arora, C., 2020. Contextual diversity for active learning, in: *Computer Vision – ECCV 2020*. Springer International Publishing, Cham. volume 12361, pp. 137–153. doi:10.1007/978-3-030-58517-4_9.
- Aghdam, H.H., Gonzalez-Garcia, A., Weijer, J.v.d., López, A.M., 2019. Active learning for deep detection neural networks, in: *Proceedings of the IEEE/CVF International Conference on Computer Vision*, pp. 3672–3680.
- Angluin, D., 1988. Queries and concept learning. *Machine Learning* 2, 319–342. doi:10.1023/A:1022821128753.
- Angluin, D., 2004. Queries revisited. *Theoretical Computer Science* 313, 175–194. doi:10.1016/j.tcs.2003.11.004.
- Ardila, D., Kiraly, A.P., Bharadwaj, S., Choi, B., Reicher, J.J., Peng, L., Tse, D., Etemadi, M., Ye, W., Corrado, G., et al., 2019. End-to-end lung cancer screening with three-dimensional deep learning on low-dose chest computed tomography. *Nature medicine* 25, 954–961.
- Ash, J., Goel, S., Krishnamurthy, A., Kakade, S., 2021. Gone fishing: Neural active learning with fisher embeddings, in: *Advances in Neural Information Processing Systems*, Curran Associates, Inc.. pp. 8927–8939.
- Ash, J.T., Zhang, C., Krishnamurthy, A., Langford, J., Agarwal, A., 2020. Deep batch active learning by diverse, uncertain gradient lower bounds, in: *International Conference on Learning Representations*.
- Atzeni, A., Peter, L., Robinson, E., Blackburn, E., Althonayan, J., Alexander, D.C., Iglesias, J.E., 2022. Deep active learning for suggestive segmentation of biomedical image stacks via optimisation of dice scores and traced boundary length. *Medical Image Analysis* 81, 102549. doi:10.1016/j.media.2022.102549.
- Bai, F., Xing, X., Shen, Y., Ma, H., Meng, M.Q.H., 2022. Discrepancy-based active learning for weakly supervised bleeding segmentation in wireless capsule endoscopy images, in: Wang, L., Dou, Q., Fletcher, P.T., Speidel, S., Li, S. (Eds.), *Medical Image Computing and Computer Assisted Intervention – MICCAI 2022*, Springer Nature Switzerland, Cham. pp. 24–34. doi:10.1007/978-3-031-16452-1_3.
- Baid, U., Ghodasara, S., Mohan, S., Bilello, M., Calabrese, E., Colak, E., Farahani, K., Kalpathy-Cramer, J., Kitamura, F.C., Pati, S., et al., 2021. The rsna-asnr-miccai brats 2021 benchmark on brain tumor segmentation and radiogenomic classification. *arXiv preprint arXiv:2107.02314*.
- Bakker, T., Muckley, M., Romero-Soriano, A., Drozdal, M., Pineda, L., 2022. On learning adaptive acquisition policies for undersampled multi-coil mri reconstruction, in: *Proceedings of The 5th International Conference on Medical Imaging with Deep Learning*, PMLR. pp. 63–85.
- Bakker, T., van Hoof, H., Welling, M., 2020. Experimental design for mri by greedy policy search, in: *Advances in Neural Information Processing Systems*, Curran Associates, Inc.. pp. 18954–18966.
- Balaram, S., Nguyen, C.M., Kassim, A., Krishnaswamy, P., 2022. Consistency-based semi-supervised evidential active learning for diagnostic radiograph classification, in: Wang, L., Dou, Q., Fletcher, P.T., Speidel, S., Li, S. (Eds.), *Medical Image Computing and Computer Assisted Intervention – MICCAI 2022*, Springer Nature Switzerland, Cham. pp. 675–685. doi:10.1007/978-3-031-16431-6_64.
- Baltruschat, I.M., Nickisch, H., Grass, M., Knopp, T., Saalbach, A., 2019. Comparison of deep learning approaches for multi-label chest x-ray classification. *Scientific reports* 9, 6381.
- Beluch, W.H., Genewein, T., Nürnberger, A., Köhler, J.M., 2018. The power of ensembles for active learning in image classification, in: *Proceedings of the IEEE Conference on Computer Vision and Pattern Recognition*, pp. 9368–9377.
- Bengar, J.Z., van de Weijer, J., Fuentes, L.L., Raducanu, B., 2022. Class-balanced active learning for image classification, in: *Proceedings of the IEEE/CVF Winter Conference on Applications of Computer Vision*, pp. 1536–1545.
- Bengar, J.Z., van de Weijer, J., Twardowski, B., Raducanu, B., 2021. Reducing label effort: Self-supervised meets active learning, in: *Proceedings of the IEEE/CVF International Conference on Computer Vision*, pp. 1631–1639.
- Van den Bergh, M., Boix, X., Roig, G., De Capitani, B., Van Gool, L., 2012. Seeds: Superpixels extracted via energy-driven sampling, in: *Computer Vision–ECCV 2012: 12th European Conference on Computer Vision*, Florence, Italy, October 7-13, 2012, *Proceedings, Part VII* 12, Springer. pp. 13–26.
- Billot, B., Magdamo, C., Cheng, Y., Arnold, S.E., Das, S., Iglesias, J.E., 2023. Robust machine learning segmentation for large-scale analysis of heterogeneous clinical brain mri datasets. *Proceedings of the National Academy of Sciences* 120, e2216399120.
- Bishop, C.M., 1994. *Mixture density networks*.
- Bıyık, E., Wang, K., Anari, N., Sadigh, D., 2019. Batch active learning using determinantal point processes. *arXiv preprint arXiv:1906.07975*.
- Bommasani, R., Hudson, D.A., Adeli, E., Altman, R., Arora, S., von Arx, S., Bernstein, M.S., Bohg, J., Bosselut, A., Brunskill, E., et al., 2021. On the opportunities and risks of foundation models. *arXiv preprint arXiv:2108.07258*.
- Budd, S., Robinson, E.C., Kainz, B., 2021. A survey on active learning and human-in-the-loop deep learning for medical image analysis. *Medical Image Analysis* 71, 102062.
- Cai, L., Xu, X., Liew, J.H., Foo, C.S., 2021. Revisiting superpixels for active learning in semantic segmentation with realistic annotation costs, in: *Proceedings of the IEEE/CVF Conference on Computer Vision and Pattern Recognition*, pp. 10988–10997.
- Caramalau, R., Bhattarai, B., Kim, T.K., 2021. Sequential graph convolutional network for active learning, in: *Proceedings of the IEEE/CVF Conference on Computer Vision and Pattern Recognition*, pp. 9583–9592.
- Cardoso, T.N.C., Silva, R.M., Canuto, S., Moro, M.M., Gonçalves, M.A., 2017. Ranked batch-mode active learning. *Information Sciences* 379, 313–337. doi:10.1016/j.ins.2016.10.037.
- Casanova, A., Pinheiro, P.O., Rostamzadeh, N., Pal, C.J., 2020. Reinforced active learning for image segmentation, in: *International Conference on Learning Representations*.
- Chaudhuri, K., Kakade, S.M., Netrapalli, P., Sanghavi, S., 2015. Convergence rates of active learning for maximum likelihood estimation, in: *Advances in Neural Information Processing Systems*, Curran Associates, Inc.
- Chen, J., Xie, Y., Wang, K., Zhang, C., Vannan, M.A., Wang, B., Qian, Z., 2021. Active image synthesis for efficient labeling. *IEEE Transactions on Pattern Analysis and Machine Intelligence* 43, 3770–3781. doi:10.1109/TPAMI.2020.2993221.
- Chen, L., Bai, Y., Huang, S., Lu, Y., Wen, B., Yuille, A.L., Zhou, Z., 2023. Making your first choice: To address cold start problem in vision active learning, in: *Medical Imaging with Deep Learning*.
- Chen, T., Kornblith, S., Swersky, K., Norouzi, M., Hinton, G.E., 2020. Big self-supervised models are strong semi-supervised learners. *Advances in neural information processing systems* 33, 22243–22255.
- Chen, Y., Mancini, M., Zhu, X., Akata, Z., 2022a. Semi-supervised and unsupervised deep visual learning: A survey. *IEEE transactions on pattern analysis and machine intelligence*.

- Chen, Z., Zhang, J., Wang, P., Chen, J., Li, J., 2022b. When active learning meets implicit semantic data augmentation, in: Avidan, S., Brostow, G., Cissé, M., Farinella, G.M., Hassner, T. (Eds.), *Computer Vision – ECCV 2022*. Springer Nature Switzerland, Cham. volume 13685, pp. 56–72. doi:10.1007/978-3-031-19806-9_4.
- Choi, J., Elezi, I., Lee, H.J., Farabet, C., Alvarez, J.M., 2021a. Active learning for deep object detection via probabilistic modeling, in: *Proceedings of the IEEE/CVF International Conference on Computer Vision*, pp. 10264–10273.
- Choi, J., Yi, K.M., Kim, J., Choo, J., Kim, B., Chang, J., Gwon, Y., Chang, H.J., 2021b. Vab-al: Incorporating class imbalance and difficulty with variational bayes for active learning, in: *Proceedings of the IEEE/CVF Conference on Computer Vision and Pattern Recognition*, pp. 6749–6758.
- Citovsky, G., DeSalvo, G., Gentile, C., Karydas, L., Rajagopalan, A., Rostamizadeh, A., Kumar, S., 2021. Batch active learning at scale, in: *Advances in Neural Information Processing Systems*, Curran Associates, Inc.. pp. 11933–11944.
- Cohn, D., Atlas, L., Ladner, R., 1994. Improving generalization with active learning. *Machine Learning* 15, 201–221. doi:10.1007/BF00993277.
- Dai, C., Wang, S., Mo, Y., Angelini, E., Guo, Y., Bai, W., 2022. Suggestive annotation of brain mr images with gradient-guided sampling. *Medical Image Analysis* 77, 102373. doi:10.1016/j.media.2022.102373.
- Dai, C., Wang, S., Mo, Y., Zhou, K., Angelini, E., Guo, Y., Bai, W., 2020. Suggestive annotation of brain tumour images with gradient-guided sampling, in: Martel, A.L., Abolmaesumi, P., Stoyanov, D., Mateus, D., Zuluaga, M.A., Zhou, S.K., Racoceanu, D., Joskowicz, L. (Eds.), *Medical Image Computing and Computer Assisted Intervention – MICCAI 2020*. Springer International Publishing, Cham. volume 12264, pp. 156–165. doi:10.1007/978-3-030-59719-1_16.
- Deng, J., Dong, W., Socher, R., Li, L.J., Li, K., Fei-Fei, L., 2009. Imagenet: A large-scale hierarchical image database, in: 2009 IEEE conference on computer vision and pattern recognition, Ieee. pp. 248–255.
- Ding, Z., Han, X., Liu, P., Niethammer, M., 2021. Local temperature scaling for probability calibration, in: *Proceedings of the IEEE/CVF International Conference on Computer Vision*, pp. 6889–6899.
- Du, P., Chen, H., Zhao, S., Chai, S., Chen, H., Li, C., 2022. Contrastive active learning under class distribution mismatch. *IEEE Transactions on Pattern Analysis and Machine Intelligence*, 1–13doi:10.1109/TPAMI.2022.3188807.
- Du, P., Zhao, S., Chen, H., Chai, S., Chen, H., Li, C., 2021. Contrastive coding for active learning under class distribution mismatch, in: *Proceedings of the IEEE/CVF International Conference on Computer Vision*, pp. 8927–8936.
- Ducoffe, M., Precioso, F., 2018. Adversarial active learning for deep networks: a margin based approach. arXiv preprint arXiv:1802.09841.
- Esteva, A., Kuprel, B., Novoa, R.A., Ko, J., Swetter, S.M., Blau, H.M., Thrun, S., 2017. Dermatologist-level classification of skin cancer with deep neural networks. *nature* 542, 115–118.
- Farahani, R.Z., Hekmatfar, M., 2009. Facility location: concepts, models, algorithms and case studies. Springer Science & Business Media.
- Feige, U., 1998. A threshold of $\ln n$ for approximating set cover. *Journal of the ACM (JACM)* 45, 634–652.
- Fu, B., Cao, Z., Wang, J., Long, M., 2021. Transferable query selection for active domain adaptation, in: *Proceedings of the IEEE/CVF Conference on Computer Vision and Pattern Recognition*, pp. 7272–7281.
- Fujishige, S., 2005. Submodular functions and optimization. Elsevier.
- Gal, Y., Ghahramani, Z., 2016. Dropout as a bayesian approximation: Representing model uncertainty in deep learning, in: *international conference on machine learning*, PMLR. pp. 1050–1059.
- Gal, Y., Islam, R., Ghahramani, Z., 2017. Deep bayesian active learning with image data, in: *Proceedings of the 34th International Conference on Machine Learning*, PMLR. pp. 1183–1192.
- Gao, M., Zhang, Z., Yu, G., Arik, S.Ö., Davis, L.S., Pfister, T., 2020. Consistency-based semi-supervised active learning: Towards minimizing labeling cost, in: Vedaldi, A., Bischof, H., Brox, T., Frahm, J.M. (Eds.), *Computer Vision – ECCV 2020*. Springer International Publishing, Cham. volume 12355, pp. 510–526. doi:10.1007/978-3-030-58607-2_30.
- Gidaris, S., Singh, P., Komodakis, N., 2018. Unsupervised representation learning by predicting image rotations, in: *International Conference on Learning Representations*.
- Gissin, D., Shalev-Shwartz, S., 2019. Discriminative active learning. arXiv preprint arXiv:1907.06347.
- Gong, J., Fan, Z., Ke, Q., Rahmani, H., Liu, J., 2022. Meta agent teaming active learning for pose estimation, in: *Proceedings of the IEEE/CVF Conference on Computer Vision and Pattern Recognition*, pp. 11079–11089.
- Goodfellow, I., Pouget-Abadie, J., Mirza, M., Xu, B., Warde-Farley, D., Ozair, S., Courville, A., Bengio, Y., 2014a. Generative adversarial nets. *Advances in neural information processing systems* 27.
- Goodfellow, I.J., Shlens, J., Szegedy, C., 2014b. Explaining and harnessing adversarial examples. arXiv preprint arXiv:1412.6572.
- Guan, H., Liu, M., 2021. Domain adaptation for medical image analysis: a survey. *IEEE Transactions on Biomedical Engineering* 69, 1173–1185.
- Guo, C., Pleiss, G., Sun, Y., Weinberger, K.Q., 2017. On calibration of modern neural networks, in: *International conference on machine learning*, PMLR. pp. 1321–1330.
- Hacohen, G., Dekel, A., Weinshall, D., 2022. Active learning on a budget: Opposite strategies suit high and low budgets, in: *International Conference on Machine Learning*, PMLR. pp. 8175–8195.
- Haußmann, M., Hamprecht, F., Kandemir, M., 2019. Deep active learning with adaptive acquisition, in: *Proceedings of the 28th International Joint Conference on Artificial Intelligence*, pp. 2470–2476.
- He, K., Chen, X., Xie, S., Li, Y., Dollár, P., Girshick, R., 2022. Masked autoencoders are scalable vision learners, in: *Proceedings of the IEEE/CVF conference on computer vision and pattern recognition*, pp. 16000–16009.
- He, K., Fan, H., Wu, Y., Xie, S., Girshick, R., 2020. Momentum contrast for unsupervised visual representation learning, in: *Proceedings of the IEEE/CVF conference on computer vision and pattern recognition*, pp. 9729–9738.
- Heo, B., Lee, M., Yun, S., Choi, J.Y., 2019. Knowledge distillation with adversarial samples supporting decision boundary, in: *Proceedings of the AAAI conference on artificial intelligence*, pp. 3771–3778.
- Hiasa, Y., Otake, Y., Takao, M., Ogawa, T., Sugano, N., Sato, Y., 2020. Automated muscle segmentation from clinical ct using bayesian u-net for personalized musculoskeletal modeling. *IEEE Transactions on Medical Imaging* 39, 1030–1040. doi:10.1109/TMI.2019.2940555.
- Hochbaum, D.S., Shmoys, D.B., 1985. A best possible heuristic for the k-center problem. *Mathematics of operations research* 10, 180–184.
- Hou, J., Graham, B., Niessner, M., Xie, S., 2021. Exploring data-efficient 3d scene understanding with contrastive scene contexts, in: *Proceedings of the IEEE/CVF Conference on Computer Vision and Pattern Recognition*, pp. 15587–15597.
- Houlsby, N., Huszár, F., Ghahramani, Z., Lengyel, M., 2011. Bayesian active learning for classification and preference learning. arXiv preprint arXiv:1112.5745.
- Hu, E.J., Wallis, P., Allen-Zhu, Z., Li, Y., Wang, S., Wang, L., Chen, W., et al., 2021. Lora: Low-rank adaptation of large language models, in: *International Conference on Learning Representations*.
- Hu, Z., Bai, X., Zhang, R., Wang, X., Sun, G., Fu, H., Tai, C.L., 2022. Lidal: Inter-frame uncertainty based active learning for 3d lidar semantic segmentation, in: *European Conference on Computer Vision*, Springer. pp. 248–265.
- Huang, D., Li, J., Chen, W., Huang, J., Chai, Z., Li, G., 2023. Divide and adapt: Active domain adaptation via customized learning, in: *Proceedings of the IEEE/CVF Conference on Computer Vision and Pattern Recognition*, pp. 7651–7660.
- Huang, G., Li, Y., Pleiss, G., Liu, Z., Hopcroft, J.E., Weinberger, K.Q., 2017. Snapshot ensembles: Train 1, get m for free. arXiv preprint arXiv:1704.00109.
- Huang, S., Wang, T., Xiong, H., Huan, J., Dou, D., 2021. Semi-supervised active learning with temporal output discrepancy, in: *Proceedings of the IEEE/CVF International Conference on Computer Vision*, pp. 3447–3456.
- Huang, Y.J., Liu, W., Wang, X., Fang, Q., Wang, R., Wang, Y., Chen, H., Chen, H., Meng, D., Wang, L., 2020. Rectifying supporting regions with mixed and active supervision for rib fracture recognition. *IEEE Transactions on Medical Imaging* 39, 3843–3854. doi:10.1109/TMI.2020.3006138.
- Hwang, S., Lee, S., Kim, S., Ok, J., Kwak, S., 2022. Combating label distribution shift for active domain adaptation, in: *European Conference on Computer Vision*, Springer. pp. 549–566.
- Jaeger, S., Karargyris, A., Candemir, S., Folio, L., Siegelman, J., Callaghan, F., Xue, Z., Palaniappan, K., Singh, R.K., Antani, S., et al., 2013. Automatic tuberculosis screening using chest radiographs. *IEEE transactions on medical imaging* 33, 233–245.
- Jia, M., Tang, L., Chen, B.C., Cardie, C., Belongie, S., Hariharan, B., Lim, S.N., 2022. Visual prompt tuning, in: *European Conference on Computer*

- Vision, Springer. pp. 709–727.
- Jin, C., Guo, Z., Lin, Y., Luo, L., Chen, H., 2023a. Label-efficient deep learning in medical image analysis: Challenges and future directions. arXiv preprint arXiv:2303.12484 .
- Jin, K.H., Unser, M., Yi, K.M., 2019. Self-supervised deep active accelerated mri. arXiv preprint arXiv:1901.04547 .
- Jin, Q., Li, S., Du, X., Yuan, M., Wang, M., Song, Z., 2023b. Density-based one-shot active learning for image segmentation. *Engineering Applications of Artificial Intelligence* 126, 106805. doi:10.1016/j.engappai.2023.106805.
- Jin, Q., Yuan, M., Li, S., Wang, H., Wang, M., Song, Z., 2022a. Cold-start active learning for image classification. *Information Sciences* 616, 16–36. doi:10.1016/j.ins.2022.10.066.
- Jin, Q., Yuan, M., Qiao, Q., Song, Z., 2022b. One-shot active learning for image segmentation via contrastive learning and diversity-based sampling. *Knowledge-Based Systems* 241, 108278. doi:10.1016/j.knosys.2022.108278.
- Jin, Q., Yuan, M., Wang, H., Wang, M., Song, Z., 2022c. Deep active learning models for imbalanced image classification. *Knowledge-Based Systems* 257, 109817. doi:10.1016/j.knosys.2022.109817.
- Joshi, A.J., Porikli, F., Papanikolopoulos, N., 2009. Multi-class active learning for image classification, in: 2009 IEEE Conference on Computer Vision and Pattern Recognition, pp. 2372–2379. doi:10.1109/CVPR.2009.5206627.
- Jung, S., Kim, S., Lee, J., 2023. A simple yet powerful deep active learning with snapshots ensembles, in: International Conference on Learning Representations.
- Karamcheti, S., Krishna, R., Fei-Fei, L., Manning, C., 2021. Mind your outliers! investigating the negative impact of outliers on active learning for visual question answering, in: Proceedings of the 59th Annual Meeting of the Association for Computational Linguistics and the 11th International Joint Conference on Natural Language Processing (Volume 1: Long Papers), Association for Computational Linguistics, Online. pp. 7265–7281. doi:10.18653/v1/2021.acl-long.564.
- Kasarla, T., Nagendar, G., Hegde, G.M., Balasubramanian, V., Jawahar, C., 2019. Region-based active learning for efficient labeling in semantic segmentation, in: 2019 IEEE Winter Conference on Applications of Computer Vision (WACV), pp. 1109–1117. doi:10.1109/WACV.2019.00123.
- Kazerouni, A., Aghdam, E.K., Heidari, M., Azad, R., Fayyaz, M., Hachaliloglu, I., Merhof, D., 2023. Diffusion models in medical imaging: A comprehensive survey. *Medical Image Analysis* , 102846.
- Kendall, A., Gal, Y., 2017. What uncertainties do we need in bayesian deep learning for computer vision? *Advances in neural information processing systems* 30.
- Kim, H., Oh, M., Hwang, S., Kwak, S., Ok, J., 2023. Adaptive superpixel for active learning in semantic segmentation, in: Proceedings of the IEEE/CVF International Conference on Computer Vision (ICCV), pp. 943–953.
- Kim, K., Park, D., Kim, K.I., Chun, S.Y., 2021. Task-aware variational adversarial active learning, in: Proceedings of the IEEE/CVF Conference on Computer Vision and Pattern Recognition, pp. 8166–8175.
- Kingma, D.P., Welling, M., 2013. Auto-encoding variational bayes. arXiv preprint arXiv:1312.6114 .
- Kirillov, A., Mintun, E., Ravi, N., Mao, H., Rolland, C., Gustafson, L., Xiao, T., Whitehead, S., Berg, A.C., Lo, W.Y., et al., 2023. Segment anything. arXiv preprint arXiv:2304.02643 .
- Kirsch, A., van Amersfoort, J., Gal, Y., 2019. Batchbald: Efficient and diverse batch acquisition for deep bayesian active learning, in: *Advances in Neural Information Processing Systems*, Curran Associates, Inc.
- Koh, P.W., Liang, P., 2017. Understanding black-box predictions via influence functions, in: International conference on machine learning, PMLR. pp. 1885–1894.
- Kohlberger, T., Singh, V., Alvino, C., Bahlmann, C., Grady, L., 2012. Evaluating segmentation error without ground truth, in: International Conference on Medical Image Computing and Computer-Assisted Intervention, Springer. pp. 528–536.
- Kothawade, S., Beck, N., Killamsetty, K., Iyer, R., 2021. Similar: Submodular information measures based active learning in realistic scenarios, in: *Advances in Neural Information Processing Systems*, Curran Associates, Inc.. pp. 18685–18697.
- Kothawade, S., Ghosh, S., Shekhar, S., Xiang, Y., Iyer, R., 2022a. Talisman: Targeted active learning for object detection with rare classes and slices using submodular mutual information, in: *Computer Vision – ECCV 2022*, Springer, Cham. pp. 1–16. doi:10.1007/978-3-031-19839-7_1.
- Kothawade, S., Kaushal, V., Ramakrishnan, G., Bilmes, J., Iyer, R., 2022b. Prism: A rich class of parameterized submodular information measures for guided data subset selection, in: *Proceedings of the AAAI Conference on Artificial Intelligence*, pp. 10238–10246.
- Kothawade, S., Savarkar, A., Iyer, V., Ramakrishnan, G., Iyer, R., 2022c. Clinical: Targeted active learning for imbalanced medical image classification, in: *Workshop on Medical Image Learning with Limited and Noisy Data*, Springer. pp. 119–129.
- Kovashka, A., Russakovsky, O., Fei-Fei, L., Grauman, K., et al., 2016. Crowdsourcing in computer vision. *Foundations and Trends® in computer graphics and Vision* 10, 177–243.
- Kuo, W., Häne, C., Yuh, E., Mukherjee, P., Malik, J., 2018. Cost-sensitive active learning for intracranial hemorrhage detection, in: Frangi, A.F., Schnabel, J.A., Davatzikos, C., Alberola-López, C., Fichtinger, G. (Eds.), *Medical Image Computing and Computer Assisted Intervention – MICCAI 2018*. Springer International Publishing, Cham. volume 11072, pp. 715–723. doi:10.1007/978-3-030-00931-1_82.
- LeCun, Y., Chopra, S., Hadsell, R., Ranzato, M., Huang, F., 2006. A tutorial on energy-based learning. *Predicting structured data* 1.
- Lee, D.H., et al., 2013. Pseudo-label: The simple and efficient semi-supervised learning method for deep neural networks, in: *Workshop on challenges in representation learning, ICML, Atlanta*. p. 896.
- Lee, K., Zlateski, A., Ashwin, V., Seung, H.S., 2015. Recursive training of 2d-3d convolutional networks for neuronal boundary prediction. *Advances in Neural Information Processing Systems* 28.
- Lewis, D.D., Catlett, J., 1994. Heterogeneous uncertainty sampling for supervised learning, in: Cohen, W.W., Hirsh, H. (Eds.), *Machine Learning Proceedings 1994*. Morgan Kaufmann, San Francisco (CA), pp. 148–156. doi:10.1016/B978-1-55860-335-6.50026-x.
- Li, H., Yin, Z., 2020. Attention, suggestion and annotation: A deep active learning framework for biomedical image segmentation, in: Martel, A.L., Abolmaesumi, P., Stoyanov, D., Mateus, D., Zuluaga, M.A., Zhou, S.K., Racoceanu, D., Joskowicz, L. (Eds.), *Medical Image Computing and Computer Assisted Intervention – MICCAI 2020*, Springer International Publishing, Cham. pp. 3–13. doi:10.1007/978-3-030-59710-8_1.
- Li, W., Li, J., Wang, Z., Polson, J., Sisk, A.E., Sajed, D.P., Speier, W., Arnold, C.W., 2022. Pathal: An active learning framework for histopathology image analysis. *IEEE Transactions on Medical Imaging* 41, 1176–1187. doi:10.1109/TMI.2021.3135002.
- Lin, Z., Wei, D., Jang, W.D., Zhou, S., Chen, X., Wang, X., Schalek, R., Berger, D., Matejek, B., Kamensky, L., Peleg, A., Haehn, D., Jones, T., Parag, T., Lichtman, J., Pfister, H., 2020. Two stream active query suggestion for active learning in connectomics, in: Vedaldi, A., Bischof, H., Brox, T., Frahm, J.M. (Eds.), *Computer Vision – ECCV 2020*, Springer International Publishing, Cham. pp. 103–120. doi:10.1007/978-3-030-58523-5_7.
- Liu, G., van Kaick, O., Huang, H., Hu, R., 2022a. Active self-training for weakly supervised 3d scene semantic segmentation. arXiv preprint arXiv:2209.07069 .
- Liu, J., Cao, L., Tian, Y., 2020. Deep active learning for effective pulmonary nodule detection, in: Martel, A.L., Abolmaesumi, P., Stoyanov, D., Mateus, D., Zuluaga, M.A., Zhou, S.K., Racoceanu, D., Joskowicz, L. (Eds.), *Medical Image Computing and Computer Assisted Intervention – MICCAI 2020*, Springer International Publishing, Cham. pp. 609–618. doi:10.1007/978-3-030-59725-2_59.
- Liu, P., Wang, L., Ranjan, R., He, G., Zhao, L., 2022b. A survey on active deep learning: from model driven to data driven. *ACM Computing Surveys (CSUR)* 54, 1–34.
- Liu, S., Yin, S., Qu, L., Wang, M., Song, Z., 2023. A structure-aware framework of unsupervised cross-modality domain adaptation via frequency and spatial knowledge distillation. *IEEE Transactions on Medical Imaging* .
- Liu, X., Zhang, F., Hou, Z., Mian, L., Wang, Z., Zhang, J., Tang, J., 2021a. Self-supervised learning: Generative or contrastive. *IEEE transactions on knowledge and data engineering* 35, 857–876.
- Liu, Z., Ding, H., Zhong, H., Li, W., Dai, J., He, C., 2021b. Influence selection for active learning, in: *Proceedings of the IEEE/CVF International Conference on Computer Vision*, pp. 9274–9283.
- Liu, Z., Wang, J., Gong, S., Lu, H., Tao, D., 2019. Deep reinforcement active learning for human-in-the-loop person re-identification, in: *Proceedings of the IEEE/CVF International Conference on Computer Vision*, pp. 6122–

- 6131.
- Lou, W., Li, H., Li, G., Han, X., Wan, X., 2023. Which pixel to annotate: A label-efficient nuclei segmentation framework. *IEEE Transactions on Medical Imaging* 42, 947–958. doi:10.1109/TMI.2022.3221666.
- Lyu, M., Zhou, J., Chen, H., Huang, Y., Yu, D., Li, Y., Guo, Y., Guo, Y., Xiang, L., Ding, G., 2023. Box-level active detection, in: *Proceedings of the IEEE/CVF Conference on Computer Vision and Pattern Recognition*, pp. 23766–23775.
- Mackowiak, R., Lenz, P., Ghorri, O., Diego, F., Lange, O., Rother, C., 2018. Ce-reals - cost-effective region-based active learning for semantic segmentation, in: *29th British Machine Vision Conference*.
- Mahapatra, D., Bozorgtabar, B., Thiran, J.P., Reyes, M., 2018. Efficient active learning for image classification and segmentation using a sample selection and conditional generative adversarial network, in: Frangi, A.F., Schnabel, J.A., Davatzikos, C., Alberola-López, C., Fichtinger, G. (Eds.), *Medical Image Computing and Computer Assisted Intervention – MICCAI 2018*. Springer International Publishing, Cham. volume 11071, pp. 580–588. doi:10.1007/978-3-030-00934-2_65.
- Mahapatra, D., Poellinger, A., Reyes, M., 2022. Graph node based interpretability guided sample selection for active learning. *IEEE Transactions on Medical Imaging* , 1–1doi:10.1109/TMI.2022.3215017.
- Mahapatra, D., Poellinger, A., Shao, L., Reyes, M., 2021. Interpretability-driven sample selection using self supervised learning for disease classification and segmentation. *IEEE Transactions on Medical Imaging* 40, 2548–2562. doi:10.1109/TMI.2021.3061724.
- Mahmood, R., Fidler, S., Law, M.T., 2022. Low-budget active learning via wasserstein distance: An integer programming approach, in: *International Conference on Learning Representations*.
- Mehrtash, A., Wells, W.M., Tempny, C.M., Abolmaesumi, P., Kapur, T., 2020. Confidence calibration and predictive uncertainty estimation for deep medical image segmentation. *IEEE transactions on medical imaging* 39, 3868–3878.
- Menze, B.H., Jakab, A., Bauer, S., Kalpathy-Cramer, J., Farahani, K., Kirby, J., Burren, Y., Porz, N., Slotboom, J., Wiest, R., et al., 2014. The multimodal brain tumor image segmentation benchmark (brats). *IEEE transactions on medical imaging* 34, 1993–2024.
- Mi, L., Wang, H., Meirovitch, Y., Schalek, R., Turaga, S.C., Lichtman, J.W., Samuel, A.D.T., Shavit, N., 2020. Learning guided electron microscopy with active acquisition, in: Martel, A.L., Abolmaesumi, P., Stoyanov, D., Mateus, D., Zuluaga, M.A., Zhou, S.K., Racoceanu, D., Joskowicz, L. (Eds.), *Medical Image Computing and Computer Assisted Intervention – MICCAI 2020*, Springer International Publishing, Cham. pp. 77–87. doi:10.1007/978-3-030-59722-1_8.
- Miyato, T., Maeda, S.i., Koyama, M., Ishii, S., 2018. Virtual adversarial training: a regularization method for supervised and semi-supervised learning. *IEEE transactions on pattern analysis and machine intelligence* 41, 1979–1993.
- Moosavi-Dezfooli, S.M., Fawzi, A., Frossard, P., 2016. Deepfool: a simple and accurate method to fool deep neural networks, in: *Proceedings of the IEEE conference on computer vision and pattern recognition*, pp. 2574–2582.
- Munjal, P., Hayat, N., Hayat, M., Sourati, J., Khan, S., 2022. Towards robust and reproducible active learning using neural networks, in: *Proceedings of the IEEE/CVF Conference on Computer Vision and Pattern Recognition*, pp. 223–232.
- Nath, V., Yang, D., Landman, B.A., Xu, D., Roth, H.R., 2021. Diminishing uncertainty within the training pool: Active learning for medical image segmentation. *IEEE Transactions on Medical Imaging* 40, 2534–2547. doi:10.1109/TMI.2020.3048055.
- Nath, V., Yang, D., Roth, H.R., Xu, D., 2022. Warm start active learning with proxy labels and selection via semi-supervised fine-tuning, in: Wang, L., Dou, Q., Fletcher, P.T., Speidel, S., Li, S. (Eds.), *Medical Image Computing and Computer Assisted Intervention – MICCAI 2022*, Springer Nature Switzerland, Cham. pp. 297–308. doi:10.1007/978-3-031-16452-1_29.
- Nguyen, C., Huynh, M.T., Tran, M.Q., Nguyen, N.H., Jain, M., Ngo, V.D., Vo, T.D., Bui, T., Truong, S.Q.H., 2021. Goal: Gist-set online active learning for efficient chest x-ray image annotation, in: *Medical Imaging with Deep Learning*.
- Ning, K.P., Zhao, X., Li, Y., Huang, S.J., 2022. Active learning for open-set annotation, in: *Proceedings of the IEEE/CVF Conference on Computer Vision and Pattern Recognition*, pp. 41–49.
- Ning, M., Lu, D., Wei, D., Bian, C., Yuan, C., Yu, S., Ma, K., Zheng, Y., 2021. Multi-anchor active domain adaptation for semantic segmentation, in: *Proceedings of the IEEE/CVF International Conference on Computer Vision*, pp. 9112–9122.
- Noroozi, M., Favaro, P., 2016. Unsupervised learning of visual representations by solving jigsaw puzzles, in: *European conference on computer vision*, Springer. pp. 69–84.
- OpenAI, 2023. Gpt-4 technical report. [arXiv:2303.08774](https://arxiv.org/abs/2303.08774).
- Park, Y., Kim, S., Choi, W., Han, D.J., Moon, J., 2023. Active learning for object detection with evidential deep learning and hierarchical uncertainty aggregation, in: *International Conference on Learning Representations*.
- Parvaneh, A., Abbasnejad, E., Teney, D., Haffari, G.R., van den Hengel, A., Shi, J.Q., 2022. Active learning by feature mixing, in: *Proceedings of the IEEE/CVF Conference on Computer Vision and Pattern Recognition*, pp. 12237–12246.
- Payer, C., Štern, D., Bischof, H., Urschler, M., 2019. Integrating spatial configuration into heatmap regression based cnns for landmark localization. *Medical image analysis* 54, 207–219.
- Peng, F., Wang, C., Liu, J., Yang, Z., 2021. Active learning for lane detection: A knowledge distillation approach, in: *Proceedings of the IEEE/CVF International Conference on Computer Vision*, pp. 15152–15161.
- Pineda, L., Basu, S., Romero, A., Calandra, R., Drozdal, M., 2020. Active mr k-space sampling with reinforcement learning, in: Martel, A.L., Abolmaesumi, P., Stoyanov, D., Mateus, D., Zuluaga, M.A., Zhou, S.K., Racoceanu, D., Joskowicz, L. (Eds.), *Medical Image Computing and Computer Assisted Intervention – MICCAI 2020*, Springer International Publishing, Cham. pp. 23–33. doi:10.1007/978-3-030-59713-9_3.
- Pourahmadi, K., Nooralinejad, P., Pirsiavash, H., 2021. A simple baseline for low-budget active learning. *arXiv preprint arXiv:2110.12033* .
- Prabhu, V., Chandrasekaran, A., Saenko, K., Hoffman, J., 2021. Active domain adaptation via clustering uncertainty-weighted embeddings, in: *Proceedings of the IEEE/CVF International Conference on Computer Vision*, pp. 8505–8514.
- Qi, Q., Li, Y., Wang, J., Zheng, H., Huang, Y., Ding, X., Rohde, G.K., 2019. Label-efficient breast cancer histopathological image classification. *IEEE Journal of Biomedical and Health Informatics* 23, 2108–2116. doi:10.1109/JBHI.2018.2885134.
- Qin, C., Schlemper, J., Caballero, J., Price, A.N., Hajnal, J.V., Rueckert, D., 2018. Convolutional recurrent neural networks for dynamic mr image reconstruction. *IEEE transactions on medical imaging* 38, 280–290.
- Qu, L., Liu, S., Liu, X., Wang, M., Song, Z., 2022. Towards label-efficient automatic diagnosis and analysis: a comprehensive survey of advanced deep learning-based weakly-supervised, semi-supervised and self-supervised techniques in histopathological image analysis. *Physics in Medicine & Biology* .
- Qu, L., Ma, Y., Yang, Z., Wang, M., Song, Z., 2023. Openal: An efficient deep active learning framework for open-set pathology image classification, in: *International Conference on Medical Image Computing and Computer-Assisted Intervention*, Springer. pp. 3–13.
- Quan, Q., Yao, Q., Li, J., Zhou, S.K., 2022. Which images to label for few-shot medical landmark detection?, in: *Proceedings of the IEEE/CVF Conference on Computer Vision and Pattern Recognition*, pp. 20606–20616.
- Radford, A., Kim, J.W., Hallacy, C., Ramesh, A., Goh, G., Agarwal, S., Sastry, G., Askell, A., Mishkin, P., Clark, J., et al., 2021. Learning transferable visual models from natural language supervision, in: *International conference on machine learning*, PMLR. pp. 8748–8763.
- Rädsch, T., Reinke, A., Weru, V., Tizabi, M.D., Schreck, N., Kavur, A.E., Pekdemir, B., Roß, T., Kopp-Schneider, A., Maier-Hein, L., 2023. Labelling instructions matter in biomedical image analysis. *Nature Machine Intelligence* 5, 273–283.
- Rajpurkar, P., Chen, E., Banerjee, O., Topol, E.J., 2022. Ai in health and medicine. *Nature medicine* 28, 31–38.
- Rangwani, H., Jain, A., Aithal, S.K., Babu, R.V., 2021. S3vaada: Submodular subset selection for virtual adversarial active domain adaptation, in: *Proceedings of the IEEE/CVF International Conference on Computer Vision*, pp. 7516–7525.
- Ren, P., Xiao, Y., Chang, X., Huang, P.Y., Li, Z., Gupta, B.B., Chen, X., Wang, X., 2021. A survey of deep active learning. *ACM computing surveys (CSUR)* 54, 1–40.
- Rombach, R., Blattmann, A., Lorenz, D., Esser, P., Ommer, B., 2022. High-resolution image synthesis with latent diffusion models, in: *Proceedings of*

- the IEEE/CVF conference on computer vision and pattern recognition, pp. 10684–10695.
- Roth, D., Small, K., 2006. Margin-based active learning for structured output spaces, in: Hutchison, D., Kanade, T., Kittler, J., Kleinberg, J.M., Mattern, F., Mitchell, J.C., Naor, M., Nierstrasz, O., Pandu Rangan, C., Steffen, B., Sudan, M., Terzopoulos, D., Tygar, D., Vardi, M.Y., Weikum, G., Fürnkranz, J., Scheffer, T., Spiliopoulou, M. (Eds.), *Machine Learning: ECML 2006*. Springer Berlin Heidelberg, Berlin, Heidelberg. volume 4212, pp. 413–424. doi:10.1007/11871842_40.
- Sadafi, A., Koehler, N., Makhro, A., Bogdanova, A., Navab, N., Marr, C., Peng, T., 2019. Multiclass deep active learning for detecting red blood cell subtypes in brightfield microscopy, in: Shen, D., Liu, T., Peters, T.M., Staib, L.H., Essert, C., Zhou, S., Yap, P.T., Khan, A. (Eds.), *Medical Image Computing and Computer Assisted Intervention – MICCAI 2019*, Springer International Publishing, Cham. pp. 685–693. doi:10.1007/978-3-030-32239-7_76.
- Sadafi, A., Navab, N., Marr, C., 2023. Active learning enhances classification of histopathology whole slide images with attention-based multiple instance learning, in: *2023 IEEE 20th International Symposium on Biomedical Imaging (ISBI)*, pp. 1–5. doi:10.1109/ISBI53787.2023.10230685.
- Saquil, Y., Kim, K.I., Hall, P., 2018. Ranking cgans: Subjective control over semantic image attributes. arXiv preprint arXiv:1804.04082 .
- Sener, O., Savarese, S., 2018. Active learning for convolutional neural networks: A core-set approach, in: *International Conference on Learning Representations*.
- Sensoy, M., Kaplan, L., Kandemir, M., 2018. Evidential deep learning to quantify classification uncertainty. *Advances in neural information processing systems* 31.
- Settles, B., 2009. Active learning literature survey .
- Seung, H.S., Opper, M., Sompolinsky, H., 1992. Query by committee, in: *Proceedings of the Fifth Annual Workshop on Computational Learning Theory, Association for Computing Machinery*, New York, NY, USA. pp. 287–294. doi:10.1145/130385.130417.
- Shaham, T.R., Dekel, T., Michaeli, T., 2019. Singan: Learning a generative model from a single natural image, in: *Proceedings of the IEEE/CVF international conference on computer vision*, pp. 4570–4580.
- Shen, H., Tian, K., Dong, P., Zhang, J., Yan, K., Che, S., Yao, J., Luo, P., Han, X., 2020. Deep active learning for breast cancer segmentation on immunohistochemistry images, in: Martel, A.L., Abolmaesumi, P., Stoyanov, D., Mateus, D., Zuluaga, M.A., Zhou, S.K., Racoceanu, D., Joskowicz, L. (Eds.), *Medical Image Computing and Computer Assisted Intervention – MICCAI 2020*, Springer International Publishing, Cham. pp. 509–518. doi:10.1007/978-3-030-59722-1_49.
- Shin, I., Kim, D.J., Cho, J.W., Woo, S., Park, K., Kweon, I.S., 2021. Labor: Labeling only if required for domain adaptive semantic segmentation, in: *Proceedings of the IEEE/CVF International Conference on Computer Vision*, pp. 8588–8598.
- Shui, C., Zhou, F., Gagné, C., Wang, B., 2020. Deep active learning: Unified and principled method for query and training, in: *Proceedings of the Twenty Third International Conference on Artificial Intelligence and Statistics*, PMLR. pp. 1308–1318.
- Siddiqui, Y., Valentin, J., Niessner, M., 2020. Viewal: Active learning with viewpoint entropy for semantic segmentation, in: *2020 IEEE/CVF Conference on Computer Vision and Pattern Recognition (CVPR)*, IEEE, Seattle, WA, USA. pp. 9430–9440. doi:10.1109/CVPR42600.2020.00945.
- Sim, Y., Chung, M.J., Kotter, E., Yune, S., Kim, M., Do, S., Han, K., Kim, H., Yang, S., Lee, D.J., et al., 2020. Deep convolutional neural network–based software improves radiologist detection of malignant lung nodules on chest radiographs. *Radiology* 294, 199–209.
- Sinha, S., Ebrahimi, S., Darrell, T., 2019. Variational adversarial active learning, in: *Proceedings of the IEEE/CVF International Conference on Computer Vision*, pp. 5972–5981.
- Sourati, J., Akcakaya, M., Leen, T.K., Erdogmus, D., Dy, J.G., 2017. Asymptotic analysis of objectives based on fisher information in active learning. *The Journal of Machine Learning Research* 18, 1123–1163.
- Sourati, J., Gholipour, A., Dy, J.G., Kurugol, S., Warfield, S.K., 2018. Active deep learning with fisher information for patch-wise semantic segmentation, in: Stoyanov, D., Taylor, Z., Carneiro, G., Syeda-Mahmood, T., Martel, A., Maier-Hein, L., Tavares, J.M.R., Bradley, A., Papa, J.P., Belagiannis, V., Nascimento, J.C., Lu, Z., Conjeti, S., Moradi, M., Greenspan, H., Madabhushi, A. (Eds.), *Deep Learning in Medical Image Analysis and Multimodal Learning for Clinical Decision Support*. Springer International Publishing, Cham. volume 11045, pp. 83–91. doi:10.1007/978-3-030-00889-5_10.
- Sourati, J., Gholipour, A., Dy, J.G., Tomas-Fernandez, X., Kurugol, S., Warfield, S.K., 2019. Intelligent labeling based on fisher information for medical image segmentation using deep learning. *IEEE Transactions on Medical Imaging* 38, 2642–2653. doi:10.1109/TMI.2019.2907805.
- Su, J.C., Tsai, Y.H., Sohn, K., Liu, B., Maji, S., Chandraker, M., 2020. Active adversarial domain adaptation, in: *Proceedings of the IEEE/CVF Winter Conference on Applications of Computer Vision*, pp. 739–748.
- Sun, S., Zhi, S., Heikkilä, J., Liu, L., 2023. Evidential uncertainty and diversity guided active learning for scene graph generation, in: *The Eleventh International Conference on Learning Representations*.
- Tajbakhsh, N., Jeyaseelan, L., Li, Q., Chiang, J.N., Wu, Z., Ding, X., 2020. Embracing imperfect datasets: A review of deep learning solutions for medical image segmentation. *Medical Image Analysis* 63, 101693.
- Takezoe, R., Liu, X., Mao, S., Chen, M.T., Feng, Z., Zhang, S., Wang, X., et al., 2023. Deep active learning for computer vision: Past and future. *APSIPA Transactions on Signal and Information Processing* 12.
- Tang, C., Xie, L., Zhang, G., Zhang, X., Tian, Q., Hu, X., 2022. Active pointly-supervised instance segmentation, in: *European Conference on Computer Vision*, Springer. pp. 606–623.
- Tarvainen, A., Valpola, H., 2017. Mean teachers are better role models: Weight-averaged consistency targets improve semi-supervised deep learning results. *Advances in neural information processing systems* 30.
- Tolkach, Y., Dohmgörge, T., Toma, M., Kristiansen, G., 2020. High-accuracy prostate cancer pathology using deep learning. *Nature Machine Intelligence* 2, 411–418.
- Tran, T., Do, T.T., Reid, I., Carneiro, G., 2019. Bayesian generative active deep learning, in: *Proceedings of the 36th International Conference on Machine Learning*, PMLR. pp. 6295–6304.
- Tschandl, P., Rinner, C., Apalla, Z., Argenziano, G., Codella, N., Halpern, A., Janda, M., Lallas, A., Longo, C., Malvehy, J., et al., 2020. Human–computer collaboration for skin cancer recognition. *Nature Medicine* 26, 1229–1234.
- Unnikrishnan, B., Nguyen, C., Balaram, S., Li, C., Foo, C.S., Krishnaswamy, P., 2021. Semi-supervised classification of radiology images with noteacher: A teacher that is not mean. *Medical Image Analysis* 73, 102148.
- Vo, H.V., Siméoni, O., Gidaris, S., Bursuc, A., Pérez, P., Ponce, J., 2022. Active learning strategies for weakly-supervised object detection, in: *European Conference on Computer Vision*, Springer. pp. 211–230.
- Wan, F., Ye, Q., Yuan, T., Xu, S., Liu, J., Ji, X., Huang, Q., 2023. Multiple instance differentiation learning for active object detection. *IEEE Transactions on Pattern Analysis and Machine Intelligence* , 1–15doi:10.1109/TPAMI.2023.3277738.
- Wang, C., Shang, K., Zhang, H., Zhao, S., Liang, D., Zhou, S.K., 2022a. Active ct reconstruction with a learned sampling policy. arXiv preprint arXiv:2211.01670 .
- Wang, J., Yan, Y., Zhang, Y., Cao, G., Yang, M., Ng, M.K., 2020a. Deep reinforcement active learning for medical image classification, in: Martel, A.L., Abolmaesumi, P., Stoyanov, D., Mateus, D., Zuluaga, M.A., Zhou, S.K., Racoceanu, D., Joskowicz, L. (Eds.), *Medical Image Computing and Computer Assisted Intervention – MICCAI 2020*, Springer International Publishing, Cham. pp. 33–42. doi:10.1007/978-3-030-59710-8_4.
- Wang, K., Zhang, D., Li, Y., Zhang, R., Lin, L., 2017. Cost-effective active learning for deep image classification. *IEEE Transactions on Circuits and Systems for Video Technology* 27, 2591–2600. doi:10.1109/TCSVT.2016.2589879.
- Wang, P., Xiao, X., Glissen Brown, J.R., Berzin, T.M., Tu, M., Xiong, F., Hu, X., Liu, P., Song, Y., Zhang, D., et al., 2018. Development and validation of a deep-learning algorithm for the detection of polyps during colonoscopy. *Nature biomedical engineering* 2, 741–748.
- Wang, S., Li, Y., Ma, K., Ma, R., Guan, H., Zheng, Y., 2020b. Dual adversarial network for deep active learning, in: Vedaldi, A., Bischof, H., Brox, T., Frahm, J.M. (Eds.), *Computer Vision – ECCV 2020*, Springer International Publishing, Cham. pp. 680–696. doi:10.1007/978-3-030-58586-0_40.
- Wang, S., Tarroni, G., Qin, C., Mo, Y., Dai, C., Chen, C., Glocker, B., Guo, Y., Rueckert, D., Bai, W., 2020c. Deep generative model-based quality control for cardiac mri segmentation, in: *Medical Image Computing and Computer Assisted Intervention–MICCAI 2020: 23rd International Conference, Lima, Peru, October 4–8, 2020, Proceedings, Part IV 23*, Springer. pp. 88–97.

- Wang, T., Li, X., Yang, P., Hu, G., Zeng, X., Huang, S., Xu, C.Z., Xu, M., 2022b. Boosting active learning via improving test performance. Proceedings of the AAAI Conference on Artificial Intelligence 36, 8566–8574. doi:10.1609/aaai.v36i8.20834.
- Wang, X., Lian, L., Yu, S.X., 2022c. Unsupervised selective labeling for more effective semi-supervised learning, in: European Conference on Computer Vision, Springer. pp. 427–445.
- Wang, Y., Huang, G., Song, S., Pan, X., Xia, Y., Wu, C., 2021. Regularizing deep networks with semantic data augmentation. IEEE Transactions on Pattern Analysis and Machine Intelligence 44, 3733–3748.
- Wang, Z., Yin, Z., 2021. Annotation-efficient cell counting, in: de Bruijne, M., Cattin, P.C., Cotin, S., Padoy, N., Speidel, S., Zheng, Y., Essert, C. (Eds.), Medical Image Computing and Computer Assisted Intervention – MICCAI 2021, Springer International Publishing, Cham. pp. 405–414. doi:10.1007/978-3-030-87237-3_39.
- Wei, K., Iyer, R., Bilmes, J., 2015. Submodularity in data subset selection and active learning, in: Proceedings of the 32nd International Conference on Machine Learning, PMLR. pp. 1954–1963.
- Williams, R.J., 1992. Simple statistical gradient-following algorithms for connectionist reinforcement learning. Machine learning 8, 229–256.
- Wu, J., Chen, J., Huang, D., 2022a. Entropy-based active learning for object detection with progressive diversity constraint, in: Proceedings of the IEEE/CVF Conference on Computer Vision and Pattern Recognition, pp. 9397–9406.
- Wu, T.H., Liou, Y.S., Yuan, S.J., Lee, H.Y., Chen, T.I., Huang, K.C., Hsu, W.H., 2022b. D2ada: Dynamic density-aware active domain adaptation for semantic segmentation, in: European Conference on Computer Vision, Springer. pp. 449–467.
- Wu, T.H., Liu, Y.C., Huang, Y.K., Lee, H.Y., Su, H.T., Huang, P.C., Hsu, W.H., 2021a. Redal: Region-based and diversity-aware active learning for point cloud semantic segmentation, in: Proceedings of the IEEE/CVF International Conference on Computer Vision, pp. 15510–15519.
- Wu, X., Chen, C., Zhong, M., Wang, J., Shi, J., 2021b. Covid-al: The diagnosis of covid-19 with deep active learning. Medical Image Analysis 68, 101913. doi:10.1016/j.media.2020.101913.
- Wu, Y., Zheng, B., Chen, J., Chen, D.Z., Wu, J., 2022c. Self-learning and one-shot learning based single-slice annotation for 3d medical image segmentation, in: Wang, L., Dou, Q., Fletcher, P.T., Speidel, S., Li, S. (Eds.), Medical Image Computing and Computer Assisted Intervention – MICCAI 2022, Springer Nature Switzerland, Cham. pp. 244–254. doi:10.1007/978-3-031-16452-1_24.
- Xie, B., Yuan, L., Li, S., Liu, C.H., Cheng, X., 2022a. Towards fewer annotations: Active learning via region impurity and prediction uncertainty for domain adaptive semantic segmentation, in: Proceedings of the IEEE/CVF Conference on Computer Vision and Pattern Recognition, pp. 8068–8078.
- Xie, B., Yuan, L., Li, S., Liu, C.H., Cheng, X., Wang, G., 2022b. Active learning for domain adaptation: An energy-based approach, in: Proceedings of the AAAI Conference on Artificial Intelligence, pp. 8708–8716. doi:10.1609/aaai.v36i8.20850.
- Xie, M., Li, S., Zhang, R., Liu, C.H., 2022c. Dirichlet-based uncertainty calibration for active domain adaptation, in: The Eleventh International Conference on Learning Representations.
- Xie, M., Li, Y., Wang, Y., Luo, Z., Gan, Z., Sun, Z., Chi, M., Wang, C., Wang, P., 2022d. Learning distinctive margin toward active domain adaptation, in: Proceedings of the IEEE/CVF Conference on Computer Vision and Pattern Recognition, pp. 7993–8002.
- Xie, Y., Ding, M., Tomizuka, M., Zhan, W., 2023a. Towards free data selection with general-purpose models, in: Thirty-seventh Conference on Neural Information Processing Systems. URL: <https://openreview.net/forum?id=KBXcDAaZE7>.
- Xie, Y., Lu, H., Yan, J., Yang, X., Tomizuka, M., Zhan, W., 2023b. Active fine-tuning: Exploiting annotation budget in the pretraining-finetuning paradigm, in: Proceedings of the IEEE/CVF Conference on Computer Vision and Pattern Recognition, pp. 23715–23724.
- Xu, X., Lu, Q., Yang, L., Hu, S., Chen, D., Hu, Y., Shi, Y., 2018. Quantization of fully convolutional networks for accurate biomedical image segmentation, in: Proceedings of the IEEE conference on computer vision and pattern recognition, pp. 8300–8308.
- Xu, Y., Xu, X., Jin, L., Gao, S., Goh, R.S.M., Ting, D.S.W., Liu, Y., 2021. Partially-supervised learning for vessel segmentation in ocular images, in: de Bruijne, M., Cattin, P.C., Cotin, S., Padoy, N., Speidel, S., Zheng, Y., Essert, C. (Eds.), Medical Image Computing and Computer Assisted Intervention – MICCAI 2021, Springer International Publishing, Cham. pp. 271–281. doi:10.1007/978-3-030-87193-2_26.
- Yang, L., Zhang, Y., Chen, J., Zhang, S., Chen, D.Z., 2017. Suggestive annotation: A deep active learning framework for biomedical image segmentation, in: Descoteaux, M., Maier-Hein, L., Franz, A., Jannin, P., Collins, D.L., Duchesne, S. (Eds.), Medical Image Computing and Computer Assisted Intervention – MICCAI 2017, Springer International Publishing, Cham. pp. 399–407. doi:10.1007/978-3-319-66179-7_46.
- Yehuda, O., Dekel, A., Hacohen, G., Weinshall, D., 2022. Active learning through a covering lens, in: Advances in Neural Information Processing Systems.
- Yi, J.S.K., Seo, M., Park, J., Choi, D.G., 2022. Pt4al: Using self-supervised pretext tasks for active learning, in: Avidan, S., Brostow, G., Cissé, M., Farinella, G.M., Hassner, T. (Eds.), Computer Vision – ECCV 2022, Springer Nature Switzerland, Cham. pp. 596–612. doi:10.1007/978-3-031-19809-0_34.
- Yoo, D., Kweon, I.S., 2019. Learning loss for active learning, in: Proceedings of the IEEE/CVF Conference on Computer Vision and Pattern Recognition, pp. 93–102.
- Yuan, J., Zhang, B., Yan, X., Chen, T., Shi, B., Li, Y., Qiao, Y., 2023. Bi3d: Bi-domain active learning for cross-domain 3d object detection, in: Proceedings of the IEEE/CVF Conference on Computer Vision and Pattern Recognition, pp. 15599–15608.
- Yuan, M., Lin, H.T., Boyd-Graber, J., 2020. Cold-start active learning through self-supervised language modeling, in: Proceedings of the 2020 Conference on Empirical Methods in Natural Language Processing (EMNLP), Association for Computational Linguistics, Online. pp. 7935–7948. doi:10.18653/v1/2020.emnlp-main.637.
- Yuan, T., Wan, F., Fu, M., Liu, J., Xu, S., Ji, X., Ye, Q., 2021. Multiple instance active learning for object detection, in: Proceedings of the IEEE/CVF Conference on Computer Vision and Pattern Recognition, pp. 5330–5339.
- Zhan, X., Wang, Q., Huang, K.h., Xiong, H., Dou, D., Chan, A.B., 2022. A comparative survey of deep active learning. arXiv preprint arXiv:2203.13450.
- Zhang, B., Li, L., Yang, S., Wang, S., Zha, Z.J., Huang, Q., 2020. State-relabeling adversarial active learning, in: Proceedings of the IEEE/CVF Conference on Computer Vision and Pattern Recognition, pp. 8756–8765.
- Zhang, B., Wang, Y., Hou, W., Wu, H., Wang, J., Okumura, M., Shinozaki, T., 2021. Flexmatch: Boosting semi-supervised learning with curriculum pseudo labeling. Advances in Neural Information Processing Systems 34, 18408–18419.
- Zhang, R., Isola, P., Efros, A.A., 2016. Colorful image colorization, in: Computer Vision—ECCV 2016: 14th European Conference, Amsterdam, The Netherlands, October 11–14, 2016, Proceedings, Part III 14, Springer. pp. 649–666.
- Zhang, W., Zhu, L., Hallinan, J., Zhang, S., Makmur, A., Cai, Q., Ooi, B.C., 2022a. Boostmis: Boosting medical image semi-supervised learning with adaptive pseudo labeling and informative active annotation, in: Proceedings of the IEEE/CVF Conference on Computer Vision and Pattern Recognition, pp. 20666–20676.
- Zhang, Y., Kang, B., Hooi, B., Yan, S., Feng, J., 2023. Deep long-tailed learning: A survey. IEEE Transactions on Pattern Analysis and Machine Intelligence.
- Zhang, Y., Zhang, X., Xie, L., Li, J., Qiu, R.C., Hu, H., Tian, Q., 2022b. One-bit active query with contrastive pairs, in: Proceedings of the IEEE/CVF Conference on Computer Vision and Pattern Recognition, pp. 9697–9705.
- Zhang, Z., Romero, A., Muckley, M.J., Vincent, P., Yang, L., Drozdal, M., 2019. Reducing uncertainty in undersampled mri reconstruction with active acquisition, in: 2019 IEEE/CVF Conference on Computer Vision and Pattern Recognition (CVPR), IEEE, Long Beach, CA, USA. pp. 2049–2053. doi:10.1109/CVPR.2019.00215.
- Zhao, Z., Zeng, Z., Xu, K., Chen, C., Guan, C., 2021. Dsal: Deeply supervised active learning from strong and weak labelers for biomedical image segmentation. IEEE Journal of Biomedical and Health Informatics 25, 3744–3751. doi:10.1109/JBHI.2021.3052320.
- Zheng, H., Yang, L., Chen, J., Han, J., Zhang, Y., Liang, P., Zhao, Z., Wang, C., Chen, D.Z., 2019. Biomedical image segmentation via representative annotation. Proceedings of the AAAI Conference on Artificial Intelligence 33, 5901–5908. doi:10.1609/aaai.v33i01.33015901.
- Zheng, H., Zhang, Y., Yang, L., Wang, C., Chen, D.Z., 2020. An annotation

- sparsification strategy for 3d medical image segmentation via representative selection and self-training. *Proceedings of the AAAI Conference on Artificial Intelligence* 34, 6925–6932. doi:[10.1609/aaai.v34i04.6175](https://doi.org/10.1609/aaai.v34i04.6175).
- Zhou, B., Khosla, A., Lapedriza, A., Oliva, A., Torralba, A., 2016. Learning deep features for discriminative localization, in: *Proceedings of the IEEE conference on computer vision and pattern recognition*, pp. 2921–2929.
- Zhou, T., Li, L., Bredell, G., Li, J., Konukoglu, E., 2021a. Quality-aware memory network for interactive volumetric image segmentation, in: de Bruijne, M., Cattin, P.C., Cotin, S., Padoy, N., Speidel, S., Zheng, Y., Essert, C. (Eds.), *Medical Image Computing and Computer Assisted Intervention – MICCAI 2021*, Springer International Publishing, Cham. pp. 560–570. doi:[10.1007/978-3-030-87196-3_52](https://doi.org/10.1007/978-3-030-87196-3_52).
- Zhou, T., Li, L., Bredell, G., Li, J., Konukoglu, E., 2022. Volumetric memory network for interactive medical image segmentation. *Medical Image Analysis* , 102599doi:[10.1016/j.media.2022.102599](https://doi.org/10.1016/j.media.2022.102599).
- Zhou, Z., Shin, J., Zhang, L., Gurudu, S., Gotway, M., Liang, J., 2017. Fine-tuning convolutional neural networks for biomedical image analysis: Actively and incrementally, in: *Proceedings of the IEEE Conference on Computer Vision and Pattern Recognition*, pp. 7340–7351.
- Zhou, Z., Shin, J.Y., Gurudu, S.R., Gotway, M.B., Liang, J., 2021b. Active, continual fine tuning of convolutional neural networks for reducing annotation efforts. *Medical Image Analysis* 71, 101997. doi:[10.1016/j.media.2021.101997](https://doi.org/10.1016/j.media.2021.101997).
- Zhu, J.J., Bento, J., 2017. Generative adversarial active learning. *arXiv preprint arXiv:1702.07956* .